European Journal of Medicinal Chemistry 182 (2019) 111648

Contents lists available at ScienceDirect

European Journal of Medicinal Chemistry

journal homepage: http://www.elsevier.com/locate/ejmech

Research paper

Design, synthesis and biological evaluation of a new series of thiazolyl-pyrazolines as dual EGFR and HER2 inhibitors

Belgin Sever [a], Mehlika Dilek Altıntop [a, *], Mohamed O. Radwan [b, c, d], Ahmet Özdemir [a], Masami Otsuka [b, c], Mikako Fujita [c, **], Halil I. Ciftci [b, c, e, ***]

[a] Department of Pharmaceutical Chemistry, Faculty of Pharmacy, Anadolu University, Eskişehir, 26470, Turkey
[b] Department of Drug Discovery, Science Farm Ltd., Kumamoto, 862-0976, Japan
[c] Medicinal and Biological Chemistry Science Farm Joint Research Labarotary, Faculty of Life Sciences, Kumamoto University, Kumamoto, 862-0973, Japan
[d] Chemistry of Natural Compounds Department, Pharmaceutical and Drug Industries Research Division, National Research Centre, Dokki, 12622, Cairo, Egypt
[e] Stanford PULSE Institute, SLAC National Accelerator Laboratory, Menlo Park, CA 94025, USA

ARTICLE INFO

Article history:
Received 17 May 2019
Received in revised form
21 August 2019
Accepted 26 August 2019
Available online 28 August 2019

Keywords:
Thiazolyl-pyrazoline
EGFR
HER2
Apoptosis
Cancer
Molecular docking

ABSTRACT

Epidermal growth factor receptor (EGFR, also known as HER1) and HER2, prominent members of receptor tyrosine kinase (RTK) superfamily, have been reported as diagnostic or prognostic markers in tumor progression. Based on the importance of molecular hybridization of pyrazoline and thiazole scaffolds in the discovery of potent anticancer agents, new thiazolyl-pyrazoline derivatives (**3a**-**v**) were synthesized and screened for their cytotoxic effects on A549 human lung adenocarcinoma, MCF-7 human breast adenocarcinoma and A375 human melanoma cell lines. 1-(4-(4-Fluorophenyl)thiazol-2-yl)-3-(4-morpholinophenyl)-5-(4-chlorophenyl)-2-pyrazoline (**3c**),1-(4-(4-cyanophenyl)thiazol-2-yl)-3-(4-morpholinophenyl)-5-(4-chlorophenyl)-2-pyrazoline (**3f**) and 1-(4-(4-cyanophenyl)thiazol-2-yl)-3-(4-piperidinophenyl)-5-(4-chlorophenyl)-2-pyrazoline (**3q**) were found as the most potent anticancer agents against A549 and MCF-7 cell lines compared to erlotinib. Compound **3q** also showed moderate cytotoxic activity against A375 cell line. Moreover, these compounds exert a cancer cell−selective action against Jurkat cell line posing no toxicity on peripheral blood mononuclear cells (PBMCs). In order to enlighten the mechanism of action underlying anticancer activity, compounds **3c**, **3f** and **3q** were investigated for their apoptotic effects on A549 and MCF-7 cell lines and inhibitory potencies against eight different RTKs including EGFR and HER2 compared to erlotinib. The results indicated that compounds **3f** and **3q** induced apoptosis in both cell lines and showed significant EGFR inhibitory activity with IC_{50} values of 4.34 ± 0.66 μM and 4.71 ± 0.84 μM, respectively when compared with erlotinib ($IC_{50} = 0.05 \pm 0.01$ μM). Besides, compound **3f** also inhibited HER2 notably with an IC_{50} value of 2.28 ± 0.53 μM making it a dual EGFR and HER2 inhibitor. Molecular docking studies, which were conducted to support the *in vitro* assays, pointed out that compound **3f** showed high affinity into the ATP binding sites of EGFR and HER2.

© 2019 Elsevier Masson SAS. All rights reserved.

1. Introduction

Receptor tyrosine kinases (RTKs) are a subclass of tyrosine kinases that catalyse the transfer of a phosphate from ATP to a hydroxyl group of a tyrosine residue. These enzymes are involved in the regulation of diverse functions in normal cells including cell growth, motility, differentiation and metabolism. Besides, they play a crucial role in oncogenesis [1,2]. There are 58 known RTKs in human beings and they are divided into 20 subfamilies including receptors of ERBB, insulin, platelet derived growth factor (PDGF)

* Corresponding author. Department of Pharmaceutical Chemistry, Faculty of Pharmacy, Anadolu University, Eskişehir, 26470, Turkey.
** Corresponding author. Medicinal and Biological Chemistry Science Farm Joint Research Labarotary, Faculty of Life Sciences, Kumamoto University, Kumamoto, 862-0973, Japan.
*** Corresponding author. Department of Drug Discovery, Science Farm Ltd., Kumamoto, 862-0976, Japan.
E-mail addresses: mdaltintop@anadolu.edu.tr (M.D. Altıntop), mfujita@kumamoto-u.ac.jp (M. Fujita), hiciftci@kumamoto-u.ac.jp (H.I. Ciftci).

https://doi.org/10.1016/j.ejmech.2019.111648
0223-5234/© 2019 Elsevier Masson SAS. All rights reserved.

and vascular endothelial growth factor (VEGF) [3,4].

ERBB, subclass I of the RTK superfamily, consists of four members: EGFR/ERBB1/HER1, ERBB2/HER2, ERBB3/HER3 and ERBB4/HER4. All these members share a similar protein structure with an extracellular ligand binding domain, a single transmembrane helix and a cytoplasmic tyrosine-kinase-containing domain [5]. Among these members, epidermal growth factor receptor (EGFR) has been reported to play an important role in tumor growth and progression including cell proliferation, impair of apoptosis, metastasis and angiogenesis [6,7]. Furthermore, HER2 is also an important cancer biomarker but there is no identified ligand for HER2. Therefore, dimerization is required for HER2 activation and heterodimers of HER2 with another ERBB family members have attracted a great deal of attention with higher stability and more potent signaling potential. EGFR/HER2 heterodimers are usually formed and they are considered to be substantial targets for cancer therapy [7–9].

Lung cancer is the most frequently diagnosed cancer type and the leading cause of cancer related mortality in the world. It is so invasive and metastazing with two distinct pathological classes, namely small-cell lung carcinoma (SCLC) and non-small-cell lung carcinoma (NSCLC), accounting for 15% and 85% of all lung cancers, respectively [10,11].

Treatment of lung cancer depends on the type and the stage of the cancer. In general, patients with stage I-II undergo surgery to remove the tumor. On the other hand, radiation therapy is also preferred in case of medical contraindications to surgical resection. However, cancer treatment has evolved from classical chemotherapy to targeted and better tolerated therapy that aim to modulate the downstream of signaling pathways underlying tumor growth and progression [12,13]. In particular, EGFR is commonly amplified, mutated, or overexpressed in NSCLC [8]. Therefore, erlotinib, an EGFR inhibitor, has been approved as a first line therapy for EGFR mutated advanced or metastatic NSCLC, refractory NSCLC, and as a maintenance therapy for NSCLC [14]. Some small molecule EGFR inhibitors used in the treatment of NSCLC are depicted in Fig. 1. Moreover, high levels of HER2 have also been detected in NSCLC [15].

Breast cancer is the most prevalent malignant disease among women and one of the most common cancers worldwide, along with lung and colon cancers. It is also so prone to metastasize to distant sites, such as lungs, bone, liver and brain. Both locoregional and systemic therapeutic options for breast cancer have progressed considerably over the past years. Cytotoxic chemotherapy, endocrine therapy and targeted therapy are used related to the tumor biology, patient outcome and the potential response of patient. In particular, HER2 is a crucial oncogenic driver of breast cancer and it is amplified in 20–30% of all breast cancers. Patients with HER2+ breast cancers generally receive trastuzumab or other HER2 targeted therapies [16–19].

Malignant melanoma, the most aggressive form of skin cancer, is generally considered to be incurable due to the low survival rates of patients, approximately less than five years. Unless it is not detected at early stage, the available treatment options are limited owing to poor prognosis and a complex etiology. The standart cure of melanoma also consists of surgery, radiation therapy, chemotherapy, immunotherapy, and targeted therapy [20–22]. Some meta-analysis and gene-expression microarray studies reported the correlation between the overexpression of EGFR and malignant melanoma lymph node metastases, whereas some studies showed negative or low EGFR expression in human melanomas [23,24].

In recent years, a significant amount of research in medicinal chemistry has been directed to the discovery of new anticancer agents as dual EGFR and HER2 inhibitors [25–31].

Pyrazolines are five-membered heterocycles containing two adjacent nitrogen atoms and an endocyclic double bond within the ring. Among three tautomeric structures of pyrazolines, 2-pyrazoline is the most common one. Diversely substituted pyrazolines have been reported to display multifarious pharmacological activities including anticancer activity. Some pyrazoline-based cytotoxic agents also possess cancer chemopreventive properties [32–34]. Moreover, thiazole is an important scaffold with an electron-donating group (-S-) and an electron-accepting group (C=N). Thiazole-based compounds show their anticancer effects through the inhibition of different molecular targets such as RTKs, non-receptor tyrosine kinases (nRTKs), phosphatidylinositol-3-kinases (PI3Ks), serine/threonine kinases (STKs), Bcl-2 family, histone deacetylases (HDACs), tumor necrosis factor-α (TNF-α). Thiazoles are present in some antineoplastic drugs such as bleomycin, tiazofurin and dasatinib (an ATP-competitive inhibitor of SRC and ABL tyrosine kinases) [35–37]. Molecular hybridization of pyrazoline and thiazole scaffolds is a reasonable and promising approach in modern medicinal chemistry. This hybridization has also led to

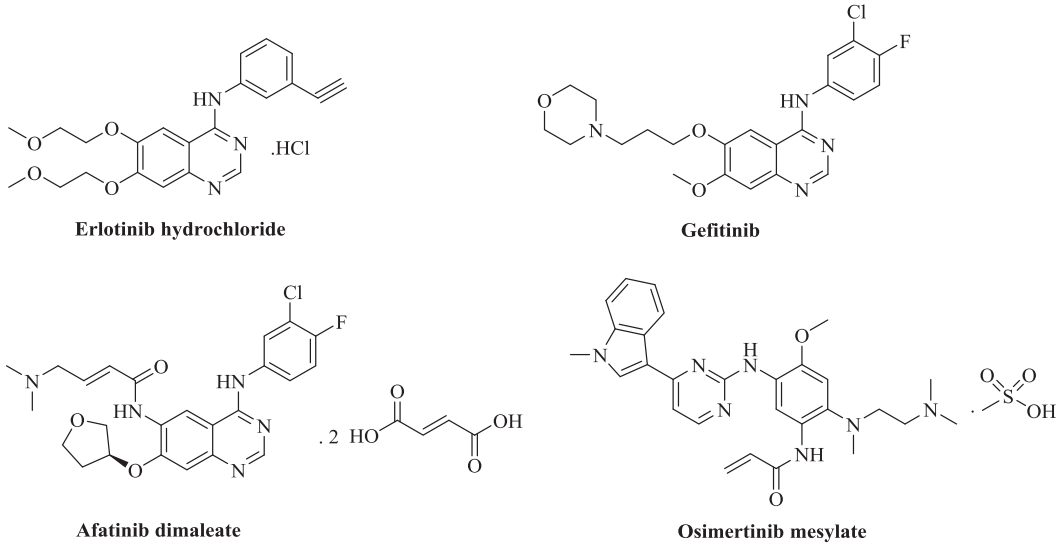

Fig. 1. Small molecule EGFR inhibitors used in the treatment of NSCLC.

the development of potent anticancer agents targeting RTKs [38–41].

In the light of the above findings, new thiazolyl-pyrazoline derivatives were designed as depicted in Fig. 2a and b, synthesized and screened for their anticancer effects on A549 human lung adenocarcinoma, MCF-7 human breast adenocarcinoma and A375 human melanoma cell lines. The tumor selectivity of the most effective compounds was also determined between Jurkat human leukemic T-cells and human peripheral blood mononuclear cells (PBMCs). Besides, the most potent anticancer agents were further investigated for their apoptotic effects on A549 and MCF-7 cell lines and inhibitory potencies against different RTKs including EGFR and HER2. Molecular docking studies were also performed in the ATP-binding sites of EGFR and HER2 to predict the possible binding modes of the most potent EGFR and HER2 inhibitors in this series.

2. Results and discussion

2.1. Chemistry

The synthesis of new thiazolyl-pyrazoline derivatives (**3a-v**) followed the general pathway outlined in Scheme 1. Initially, the base-catalyzed *Claisen-Schmidt* condensation of 4′-morpholino/piperidinoacetophenone with 4-chlorobenzaldehyde gave 3-(4-chlorophenyl)-1-(4-morpholino/piperidinophenyl)-2-propen-1-ones (**1a**/**1b**), which underwent a subsequent cyclization reaction with thiosemicarbazide in the presence of sodium hydroxide affording 3-(4-morpholino/piperidinophenyl)-5-(4-chlorophenyl)-1-thiocarbamoyl-2-pyrazolines (**2a**/**2b**). Finally, new thiazolyl-pyrazolines (**3a-v**) were synthesized *via* the ring closure reaction of compound **2a**/**2b** with 2-bromo-1-arylethanones. The structures of all synthesized compounds were elucidated by spectral data.

In the IR spectra of thiazolyl-pyrazoline derivatives (**3a-v**), the absence of NH_2 bands at 3437.15–3263.56 cm^{-1} belonging to the thiocarbamoyl moieties of compounds **2a**/**2b** confirmed the formation of the thiazole rings of compounds **3a-v**. Besides, the aromatic and aliphatic C-H stretching vibrations gave rise to the bands at 3130.47–3020.53 cm^{-1} and 2972.31–2796.78 cm^{-1}, respectively. The stretching bands for C═N and C═C groups occurred at 1606.70–1440.83 cm^{-1}. The C≡N stretching bands for compound **3f** at 2220.07 cm^{-1} and for compound **3q** at 2223.92 cm^{-1} were also observed.

In the ^{1}H NMR spectra of the pyrazolines, the characteristic doublets of doublets related to ABX system (Fig. 3) were observed in the expected regions. The H_A protons resonated as a doublet of doublets (J_{AB} = 17.40–17.85 Hz, J_{AX} = 6.33–6.87 Hz) or a multiplet at 3.20–3.36 ppm, whereas the H_B protons were observed as a doublet of doublets (J_{BA}= 17.70–17.91 Hz, J_{BX} = 11.67–11.88 Hz) at 3.97–4.02 ppm. The H_X protons appeared as a doublet of doublets at 5.60–5.67 ppm (J_{AX} = 6.27–7.08 Hz, J_{BX} = 11.22–11.85 Hz) due to the vicinal coupling with the non-equivalent protons of the methylene group at the 4th position of the pyrazoline ring. The thiazole protons appeared as a singlet at 7.10–7.67 ppm. All the other aromatic and aliphatic protons were found in expected regions. Besides, the ^{13}C NMR chemical shift values corroborated the features of the pyrazoline and thiazole scaffolds. The C_3, C_4 and C_5 carbons of the pyrazoline ring were observed at 152.54–153.96 ppm, 43.53–43.66 ppm and 63.60–63.98 ppm, respectively. However, the C_2, C_4 and C_5 carbons of the thiazole ring appeared at 164.88–165.19 ppm, 148.81–152.70 ppm and 102.25–109.38 ppm, respectively. The absence of the thiocarbamoyl carbon peaks of compounds **2a**/**2b** (at 175.80 and 175.72 ppm, respectively) once more confirmed the formation of the thiazole rings. All the other aromatic and aliphatic carbons were observed in expected regions. Besides, the heteronuclear single-quantum coherence (HSQC) was performed for compounds **3c**, **3d** and **3g** to correlate the chemical shift values of ^{1}H NMR and ^{13}C NMR. The H_A protons at 3.25–3.34 ppm and the H_B protons at 3.99 and 4.00 ppm correlated with the C_4 carbons at 43.60–43.62 ppm, whereas the H_X protons at 5.62 and 5.63 ppm correlated with the C_5 carbons at 63.70 and 63.73 ppm. The H_1 and H_2 protons of the morpholine rings at 3.21 ppm and 3.74 ppm were found to have a correlation with the C_1 and C_2 carbons of the morpholine rings at 47.92, 47.93 ppm and 66.37 ppm, respectively (Fig. 4a). Moreover, the ^{1}H-^{1}H correlation spectroscopy (COSY) data of compound **3l** also reinforced the formation of 2-pyrazoline scaffold indicating the geminal coupling between the H_A and H_B protons and the vicinal coupling of the H_X proton with the H_A and H_B protons. The ^{1}H-^{1}H COSY of compound **3l** also exhibited the correlation between the H_1 and H_2 protons of the piperidine ring at 1.59 ppm and 3.26–3.31 ppm, respectively (Fig. 4b). Finally, the high resolution mass spectrometry (HRMS) data of all compounds were consistent

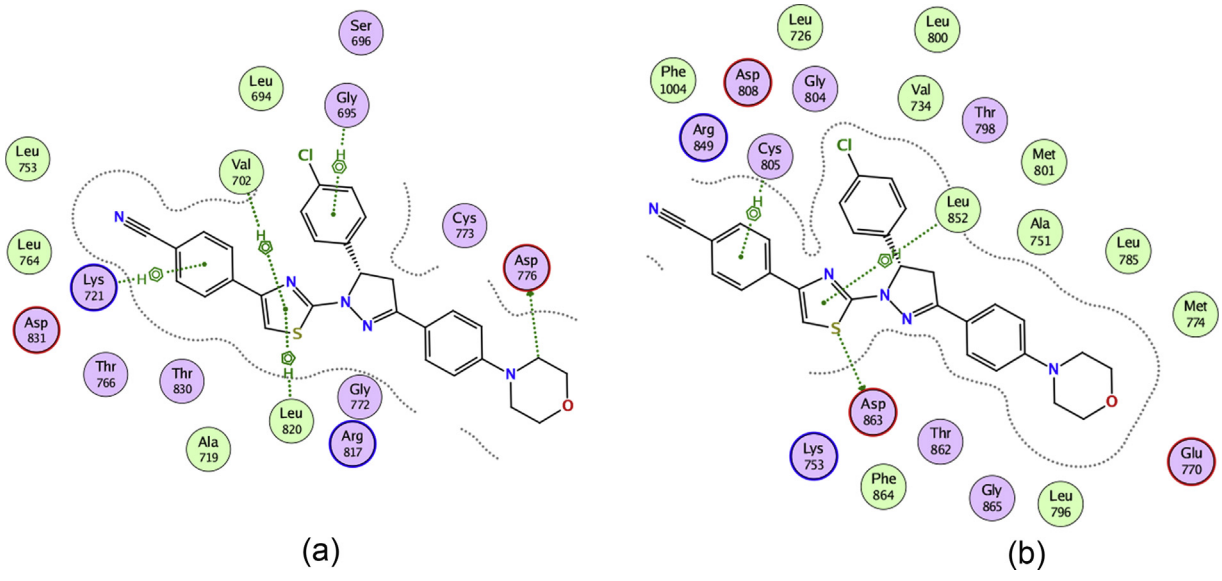

Fig. 2. 2D Depiction of binding mode of compound **3f** into EGFR (a) and HER2 (b).

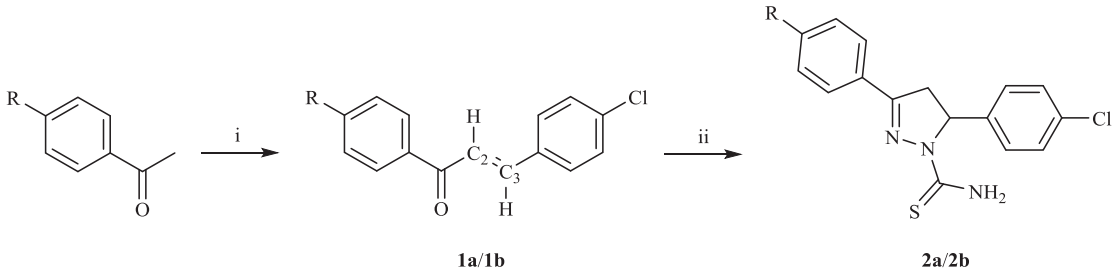

Compound	R	R'	Compound	R	R'
1a	Morpholino	-	**1b**	Piperidino	-
2a	Morpholino	-	**2b**	Piperidino	-
3a	Morpholino	Phenyl	**3l**	Piperidino	Phenyl
3b	Morpholino	4-Nitrophenyl	**3m**	Piperidino	4-Nitrophenyl
3c	Morpholino	4-Fluorophenyl	**3n**	Piperidino	4-Fluorophenyl
3d	Morpholino	4-Chlorophenyl	**3o**	Piperidino	4-Chlorophenyl
3e	Morpholino	4-Bromophenyl	**3p**	Piperidino	4-Bromophenyl
3f	Morpholino	4-Cyanophenyl	**3q**	Piperidino	4-Cyanophenyl
3g	Morpholino	4-Trifluoromethylphenyl	**3r**	Piperidino	4-Trifluoromethylphenyl
3h	Morpholino	4-Methylphenyl	**3s**	Piperidino	4-Methylphenyl
3i	Morpholino	4-Methoxyphenyl	**3t**	Piperidino	4-Methoxyphenyl
3j	Morpholino	4-Methylsulfonylphenyl	**3u**	Piperidino	4-Methylsulfonylphenyl
3k	Morpholino	Naphth-2-yl	**3v**	Piperidino	Naphth-2-yl

Scheme 1. The synthetic route for the preparation of thiazolyl-pyrazoline derivatives (**3a-v**). Reagents and conditions: (i) 4-Chlorobenzaldehyde, 40% (w/v) NaOH, ethanol, rt, 24 h; (ii) thiosemicarbazide, NaOH, ethanol, reflux, 12 h; (iii) 2-bromo-1-arylethanone, ethanol, reflux, 6 h.

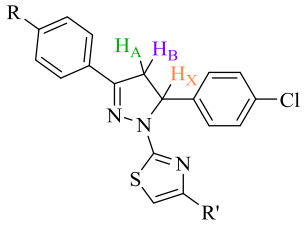

Fig. 3. ABX system of the pyrazoline ring.

with their molecular formulas.

2.2. Biological evaluation

MTT assay was carried out to determine the cytotoxic effects of the compounds on A549, MCF-7 and A375 cell lines (Table 1). Among compounds **3a**-**k**, 4-fluorophenyl substituted compound **3c** and 4-cyanophenyl substituted compound **3f** were identified as the most effective anticancer agents against A549 and MCF-7 cell lines. IC_{50} values of compounds **3c**, **3f** and erlotinib for A549 cell line were

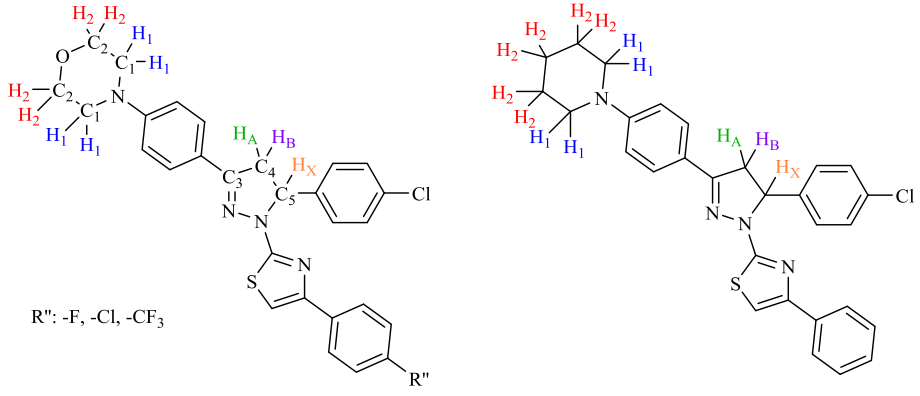

Fig. 4. Diagram for HSQC spectra of compounds **3c**, **3d** and **3g** (a) and diagram for COSY spectrum of compound **3l** (b).

Table 1
IC_{50} values of compounds **3c**, **3f**, **3q** and erlotinib against A549, MCF-7 and A375 cells.

Compound	IC_{50} (μM)		
	A549 Cell Line	MCF-7 Cell Line	A375 Cell line
2a	>100	37.42 ± 5.18	>100
2b	33.83 ± 2.78	22.33 ± 2.38	>100
3a	76.50 ± 5.95	52.10 ± 7.21	>100
3b	>100	>100	>100
3c	8.95 ± 1.43	9.59 ± 1.95	84.42 ± 11.19
3d	18.97 ± 3.27	14.92 ± 3.55	75.86 ± 13.21
3e	94.27 ± 7.34	70.64 ± 9.51	>100
3f	10.76 ± 1.81	8.05 ± 1.47	53.54 ± 7.48
3g	39.30 ± 4.22	>100	>100
3h	>100	>100	>100
3i	>100	>100	>100
3j	10.74 ± 1.15	67.16 ± 8.92	>100
3k	>100	>100	>100
3l	64.21 ± 7.48	28.43 ± 4.26	65.83 ± 8.59
3m	>100	>100	>100
3n	70.23 ± 7.19	23.11 ± 3.44	71.44 ± 9.84
3o	46.40 ± 6.08	>100	>100
3p	39.74 ± 5.33	>100	>100
3q	11.16 ± 2.12	9.76 ± 1.58	38.72 ± 5.47
3r	42.02 ± 3.46	23.66 ± 4.08	64.18 ± 10.25
3s	>100	>100	>100
3t	>100	>100	>100
3u	>100	>100	>100
3v	>100	>100	>100
Erlotinib	22.35 ± 2.84	8.24 ± 1.37	27.26 ± 6.81

determined as 8.95 ± 1.43, 10.76 ± 1.81 and 22.35 ± 2.84 μM, respectively. Moreover, IC_{50} values of compounds **3c**, **3f** and erlotinib for MCF-7 cell line were found as 9.59 ± 1.95, 8.05 ± 1.47 and 8.24 ± 1.37 μM, respectively. Besides, among compounds **3l-v**, 4-cyanophenyl substituted compound **3q** exhibited the most promising anticancer activity against A549 and MCF-7 cell lines with IC_{50} values of 11.16 ± 2.12 μM and 9.76 ± 1.58 μM, respectively. Compound **3q** also displayed moderate cytotoxic activity against A375 cell line with an IC_{50} value of 38.72 ± 5.47 μM. The anticancer effects of compounds **3c**, **3f**, **3q** were demonstrated as graphs in comparison with erlotinib at different concentrations after 72 h incubation as given in Fig. 5a and b. According to all results, it can be concluded that morpholine ring enhanced anticancer activity more than piperidine ring. The presence of the cyanophenyl moiety at the 4th position of the thiazole scaffold also increased anticancer activity, whereas 4-nitrophenyl, 4-methylphenyl, 4-methoxyphenyl and naphth-2-yl moieties at the 4th position of the thiazole ring led to a significant drop in anticancer activity. Compounds **2a** and **2b** showed less anticancer activity than compounds **3c**, **3f**, **3q** against both cell lines indicating that the formation of thiazole scaffold also enhanced anticancer activity.

Due to their significant anticancer potentials against A549 and MCF-7 cell lines, compounds **3c**, **3f** and **3q** were further investigated for the evaluation of tumor selectivity between Jurkat cells and PBMCs. The results indicated that these compounds showed significant tumor selectivity in PBMCs (approximately 10 times and more) as depicted in Table 2 and Fig. 6a and b.

The most potent anticancer agents were chosen for the assessment of apoptosis in A549 and MCF-7 cell lines using annexin V/ethidium homodimer III staining method. These cell lines were incubated with compound **3c**, **3f** and **3q** at the IC_{50} concentrations and then were stained and observed by a fluorescence microscope. According to this method, if the cells are stained red with ethidium homodimer III and not colored green with annexin V, the cells are considered to be necrotic. On the other hand, the completely opposite results indicate apoptosis. Compounds **3c**, **3f** and **3q** significantly induced apoptosis in A549 cells with 65%, 68% and 77%, respectively when compared with erlotinib (72%) as shown in Table 3 and Fig. 7. Moreover, compounds **3c**, **3f** and **3q** showed significant apoptotic activity in MCF-7 cells with 78%, 51% and 63%, respectively when compared with erlotinib (66%) (Table 3, Fig. 8).

Since RTKs have been known with their crucial roles in oncogenesis, they serve as promising molecular targets for cancer therapy. Herein, multipoint dose-response experiments were performed using eight members of RTKs (EGFR, HER2, HER4, insulin-like growth factor receptor 1 (IGF1R), insulin receptor (InsR), kinase insert domain receptor (KDR) platelet-derived growth factor receptors (PDGFRα and PDGFRβ)) to provide a mechanistic insight into anticancer potentials of compounds **3c**, **3f** and **3q**. Compounds **3f** and **3q** were found as the most potent EGFR inhibitors in this series with IC_{50} values of 4.34 ± 0.66 and 4.71 ± 0.84 μM, respectively when compared with erlotinib (0.05 ± 0.01 μM) (Table 4 and Fig. 9). Besides, compound **3f** showed significant inhibitory effect on HER2 with an IC_{50} value of 2.28 ± 0.53 μM. According to the results, compound **3f** could be defined as a promising dual EGFR and HER2 inhibitor, whereas compound **3q** only inhibited EGFR significantly. Compound **3f** also inhibited HER4 with an IC_{50} value of 4.68 ± 1.12 μM. Although compound **3c** notably inhibited HER4 and IGF1R with IC_{50} values of 1.50 ± 0.34 μM and 3.28 ± 1.41 μM, respectively, this compound did not show any significant inhibitory activity against EGFR (IC_{50} = 23.34 ± 3.26 μM). Compound **3c** also showed moderate HER2 inhibitory activity with an IC_{50} value of 6.96 ± 1.37 μM. The inhibitory effects of compounds **3c**, **3f**, **3q** and erlotinib on kinases pointed out the distinct inhibitor profiles of these compounds not only than each other but also than erlotinib as illustrated in Fig. 10.

2.3. Molecular docking studies

Molecular docking studies were conducted to explore possible binding modes of the most promising antiproliferative lead compounds in the ATP-binding site of EGFR. The co-crystal structure of EGFR with erlotinib was retrieved from protein data bank (PDB) server and selected as the docking model (PDB ID code: 4HJO) [42]. Compounds **3f** and **3q** adopted similar poses in EGFR site where the 4-cyanophenyl group forges a key H-Pi interaction with Lys721. These compounds were also anchored by their sandwiched thiazoles between Val702 and Leu820 showing a remarkable H-pi interaction. The morpholine and piperidine rings do not seem to play a significant binding role. Although compound **3f** and **3q** fit well inside the pocket, they miss crucial H-bonds with Met769 and Thr766. This outcome explains their less activity compared to erlotinib as depicted in Fig. 11a. In a similar vein, compound **3c** lacks Lys721 interaction however, its thiazole binds to Thr766 through HOH4 bridge. Furthermore, it does not exhibit the same strong H-Pi interactions with Val702 and Leu820 which explains its weaker affinity in comparison to compounds **3f** and **3q** (Fig. 11b).

Although only compound **3f** significantly inhibited HER2 according to *in vitro* enzyme studies, molecular docking studies were also carried out for compounds **3c** and **3q** in the HER2 binding site (PDB ID code: 3RCD) [43]. According to docking results, compound **3f** forms a key interaction with Asp863 but lacks a crucial bond with Met801. Compound **3f** forges substantial H-Pi interactions with Cys 805 and Leu 852 through its cyanophenyl and thiazole moieties, respectively. On the contrary, compound **3q** formed no observable intermolecular interactions (Fig. 11c). Compound **3c**, with its moderate inhibitory activity, only formed two interactions with Thr862 and Asp863 as shown in Fig. 11d.

3. Conclusion

In this paper, new thiazolyl-pyrazoline derivatives (**3a-v**) were

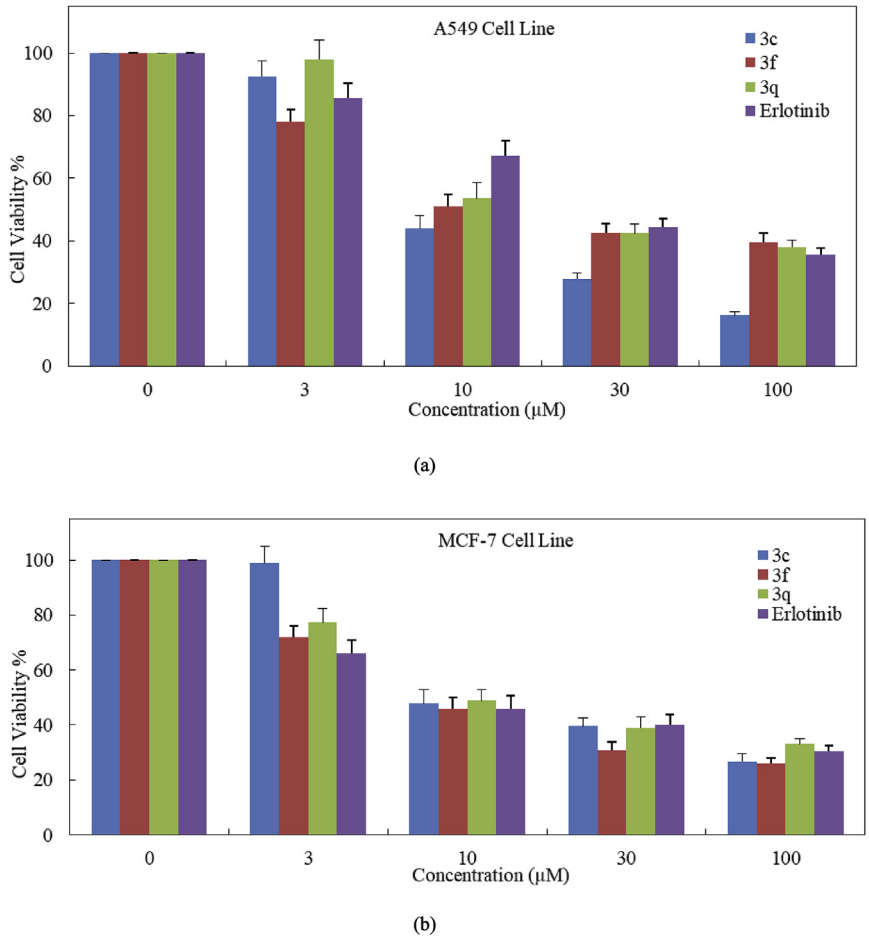

Fig. 5. Cytotoxic effects of compounds **3c**, **3f**, **3q** and erlotinib on A549 cell line (a); MCF-7 cell line (b) after 72 h incubation.

Table 2
IC_{50} values of compounds **3c**, **3f**, **3q** and erlotinib against Jurkat cells and PBMCs.

Compound	IC_{50} (μM)	
	Jurkat Cells	PBMCs
3c	23.43 ± 3.43	>300
3f	41.01 ± 5.51	299.44 ± 16.43
3q	29.48 ± 4.38	298.74 ± 14.41
Erlotinib	12.07 ± 1.47	39.32 ± 5.86

synthesized and evaluated for their anticancer effects on A549, MCF-7 and A375 cell lines. The results revealed that compounds **3c**, **3f** and **3q** displayed potent and selective anticancer activity against A549 and MCF-7 cell lines compared to erlotinib. Compounds **3c**, **3f** and **3q** also significantly induced apoptosis in both cell lines. Moreover, these compounds were investigated for their inhibitory potencies against eight kinases as compared to erlotinib. Compound **3f** showed potent EGFR and HER2 inhibitory effects, which shed light on its notable anticancer effects on A549 and MCF-7 cell lines, respectively. However, compound **3q** only exhibited notable EGFR inhibitory activity, which could be beneficial to explain its anti-lung cancer activity. Although compound **3c** was found as a potential anticancer agent against A549 and MCF-7 cell lines, it showed no significant inhibitory effect on EGFR, the most crucial target in this large panel of kinases. Compound **3c** showed notable HER4 and IGF1R inhibitory effects, which proved its different kinase inhibitor profile than compounds **3f** and **3q**. Molecular docking results were in agreement with *in vitro* biological assay data. Compounds **3f** and **3q** showed good binding affinity to ATP binding site of EGFR with proper interactions, whereas they missed the crucial H-bonds with Met769 and Thr766. Besides, compound **3f** also fitted well in the HER2 binding site lacking an important interaction with Met801. According to all *in vitro* and *in silico* studies, compound **3f** stands out as a promising dual EGFR and HER2 inhibitor and apoptosis inducer for further experiments.

4. Experimental

4.1. Chemistry

All reagents obtained from commercial suppliers were used without further purification. The melting points (M.p.) of the compounds were determined on a MP90 digital melting point apparatus (Mettler Toledo, Ohio, USA) and are uncorrected. IR spectra were determined on an IRPrestige-21 Fourier Transform Infrared spectrophotometer (Shimadzu, Tokyo, Japan). ^{1}H NMR, ^{13}C NMR, HSQC and COSY spectra were recorded on a Bruker spectrometer (Bruker, Billerica, MA, USA), whereas HRMS spectra were recorded on a Shimadzu LCMS-IT-TOF system (Shimadzu, Kyoto, Japan). Thin Layer Chromatography (TLC) was applied on TLC Silica gel 60 F_{254} aluminium sheets (Merck, Darmstadt, Germany).

4.1.1. General procedure for the synthesis of the compounds

*4.1.1.1. 3-(4-Chlorophenyl)-1-(4-morpholino/piperidinophenyl)-2-propen-1-ones (**1a**/**1b**).* A mixture of 4′-morpholino/piperidinoacetophenone (0.02 mol), 4-chlorobenzaldehyde (0.02 mol)

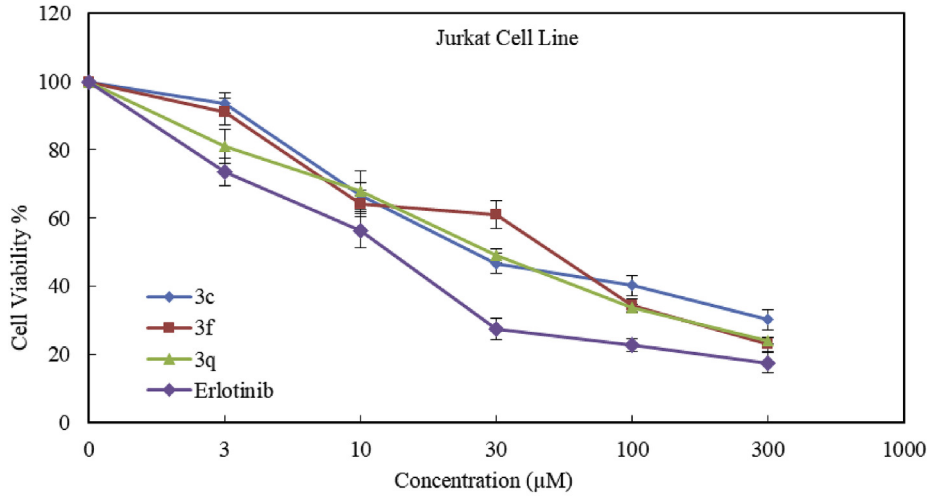

(a)

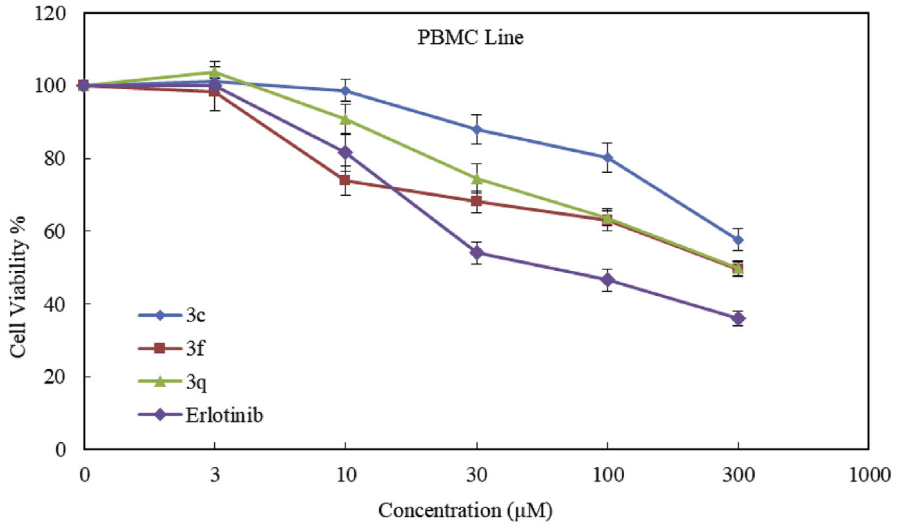

(b)

Fig. 6. Cytotoxic effects of compounds **3c**, **3f**, **3q** and erlotinib on Jurkat cells (a), and PBMCs (b) after 72 h incubation.

Table 3
Percents of apoptosis in A549 and MCF-7 cell lines treated with compounds **3c**, **3f**, **3q** and erlotinib.

Compound	A549 cell line			MCF-7 cell line		
	Apoptosis%	Late Apoptosis/Necrosis%	Necrosis%	Apoptosis%	Late Apoptosis/Necrosis%	Necrosis%
3c	65	23	12	78	14	8
3f	68	19	13	51	32	27
3q	77	15	8	63	27	10
Erlotinib	72	19	9	66	21	13

and 40% (w/v) aqueous sodium hydroxide (5 mL) in ethanol (30 mL) was stirred at room temperature for 24 h. After completion of the reaction (monitored by TLC), the reaction mixture was poured into crushed ice. The precipitated solid was filtered, washed with water, and dried. The product was crystallized from ethanol [44].

*4.1.1.1.1. 3-(4-Chlorophenyl)-1-(4-morpholinophenyl)-2-propen-1-one (**1a**).* Yield: 80%. M.p. 201.5 °C, Lit. M.p. 203–205 °C [45].

IR ν_{max} (cm^{-1}): 2968.45, 2897.08, 2850.79 (aliphatic C-H stretching), 1645.28 (C=O stretching), 1602.85, 1585.49, 1562.34, 1548.84, 1516.05, 1489.05, 1446.61 (C=C stretching), 1425.40, 1406.11, 1381.03, 1359.82, 1336.67, 1317.38, 1296.16, 1267.23, 1253.73, 1224.80, 1192.01, 1120.64, 1083.99, 1055.06, 1028.06, 1012.63 (C-H bending, C-N, C-O stretching and aromatic C-H in plane bending), 985.62, 927.76, 867.97, 812.03, 748.38, 736.81, 671.23, 640.37 (aromatic C-H out of plane bending).

^{1}H NMR (300 MHz, DMSO-d_6) δ (ppm): 3.35 (4H, brs), 3.75 (4H, t,

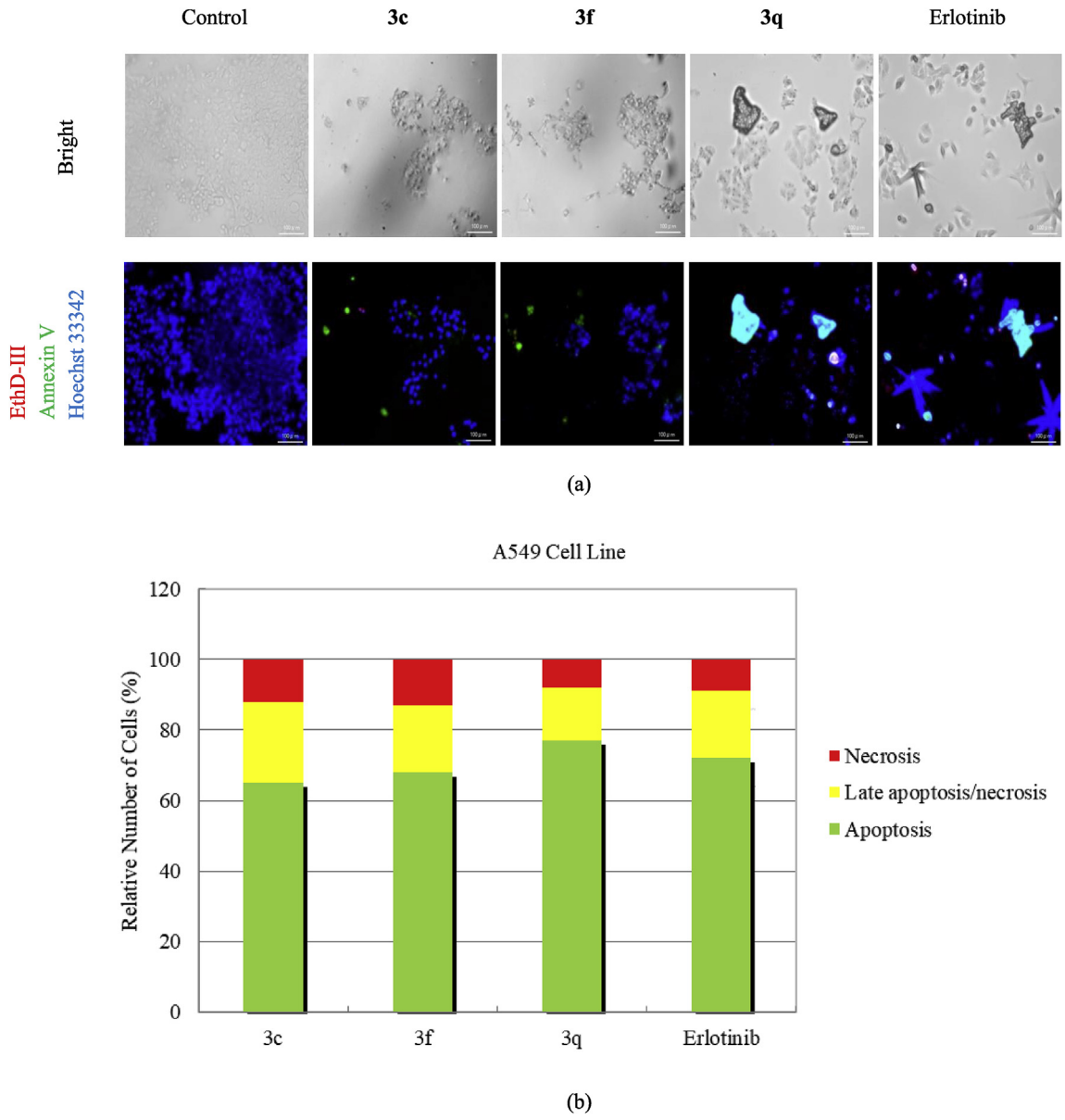

Fig. 7. Apoptotic/necrotic effects on A549 cells at IC_{50} concentrations of compounds **3c**, **3f**, **3q** and erlotinib (a) for 6 h. (b) A total of approximate 100 stained cells were selected randomly in each experiment of (a) and were classified into 3 types "apoptosis" (green), "necrosis or late apoptosis" (both green and red) and "necrosis" (red). (For interpretation of the references to color in this figure legend, the reader is referred to the Web version of this article.)

J = 4.59, 5.13, 9.72 Hz), 7.03 (2H, d, J = 9.09 Hz), 7.51 (2H, d, J = 8.55 Hz), 7.65 (1H, d, J = 15.57 Hz), 7.90–7.99 (3H, m), 8.08 (2H, d, J = 9.03 Hz).

^{13}C NMR (75 MHz, DMSO-d_6) δ (ppm): 47.14 ($2CH_2$), 66.32 ($2CH_2$), 113.51 (2CH), 123.47 (CH), 127.81 (C), 129.36 (2CH), 130.86 (2CH), 131.10 (2CH), 134.46 (C), 135.10 (C), 141.25 (CH), 154.61 (C), 186.86 (C).

HRMS (ESI) (m/z) $[M+H]^+$ calcd. for $C_{19}H_{18}ClNO_2$: 328.1099, found: 328.1103.

*4.1.1.1.2. 3-(4-Chlorophenyl)-1-(4-piperidinophenyl)-2-propen-1-one (**1b**).* Yield: 75%. *Lit.* M.p. 187.2 °C [46].

IR ν_{max} (cm^{-1}): 3184.48, 3097.68, 3037.89 (aromatic C-H stretching), 2945.30, 2827.64 (aliphatic C-H stretching), 1649.14 (C=O stretching), 1602.85, 1583.56, 1566.20, 1546.91, 1517.98, 1489.05, 1450.47 (C=C stretching), 1427.32, 1402.85, 1386.82, 1355.96, 1330.88, 1313.52, 1294.24, 1274.95, 1255.66, 1224.80, 1192.01, 1076.58, 1122.17, 1091.71, 1076.28, 1029.99, 1010.70 (C-H bending, C-N stretching and aromatic C-H in plane bending), 987.55, 916.19, 862.18, 806.25, 748.38, 734.88, 707.88, 673.16, 623.01 (aromatic C-H out of plane bending).

^{1}H NMR (300 MHz, DMSO-d_6) δ (ppm): 1.60 (6H, s), 3.41 (4H, s), 6.98 (2H, d, J = 9.15 Hz), 7.51 (2H, d, J = 8.52 Hz), 7.63 (1H, d, J = 15.60 Hz), 7.89–7.96 (3H, m), 8.04 (2H, d, J = 9.06 Hz).

^{13}C NMR (75 MHz, DMSO-d_6) δ (ppm): 24.44 (CH_2), 25.36 ($2CH_2$), 48.15 ($2CH_2$), 113.41 (2CH), 123.57 (CH), 126.58 (C), 129.34 (2CH), 130.77 (2CH), 131.29 (2CH), 134.54 (C), 134.99 (C), 140.86 (CH), 154.39 (C), 186.50 (C).

HRMS (ESI) (m/z) $[M+H]^+$ calcd. for $C_{20}H_{20}ClNO$: 326.1306, found: 326.1307.

*4.1.1.2. 3-(4-Morpholino/piperidinophenyl)-5-(4-chlorophenyl)-1-thiocarbamoyl-2-pyrazoline (**2a**/**2b**).* A mixture of chalcone (**1a**/**1b**) (0.01 mol), thiosemicarbazide (0.012 mol) and sodium hydroxide (0.025 mol) was refluxed in ethanol (25 mL) for 12 h. The product

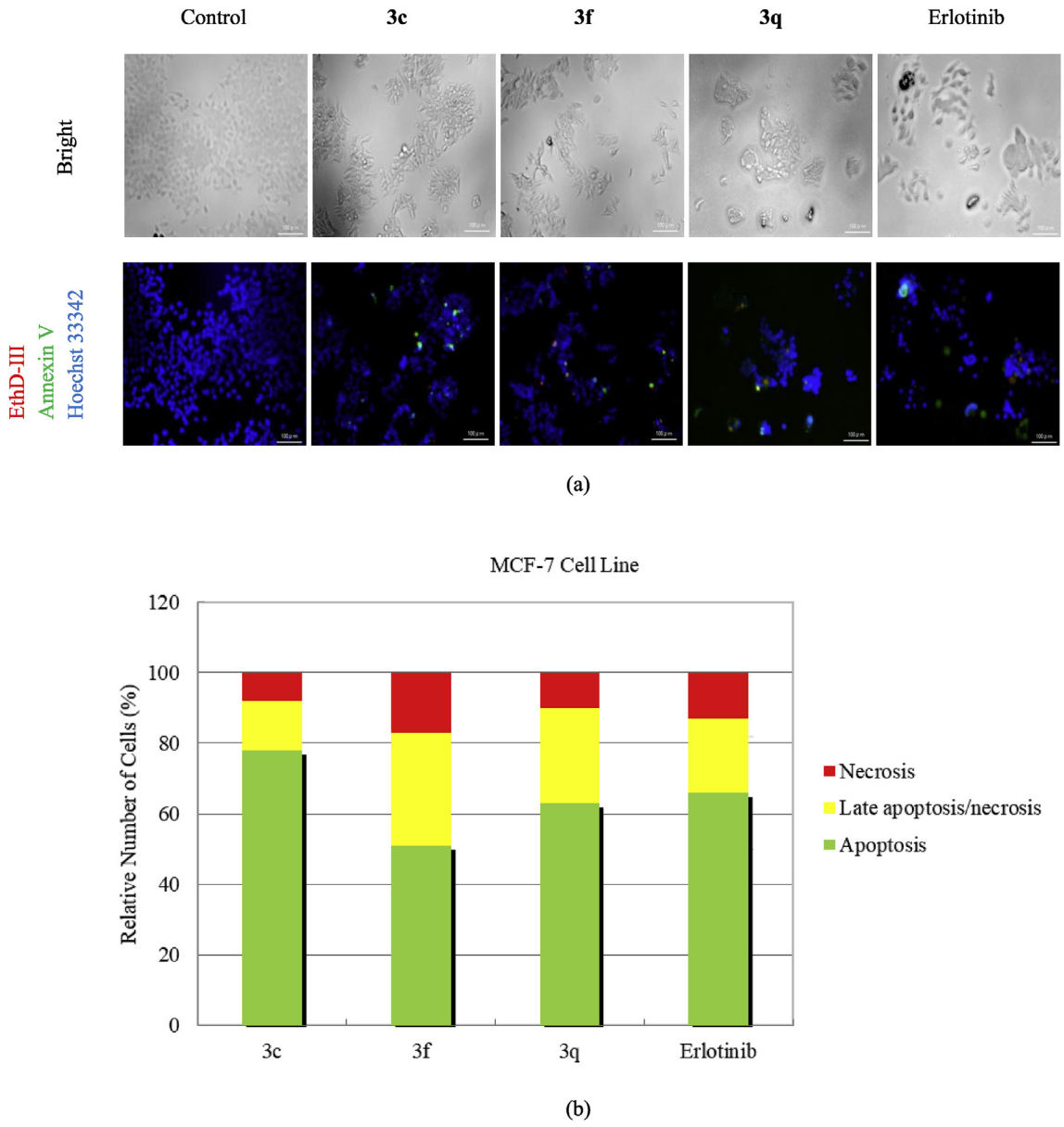

Fig. 8. Apoptotic/necrotic effects of compounds **3c**, **3f**, **3q** and erlotinib at their IC_{50} concentrations on MCF-7 cell line (a) for 6 h. (b) A total of approximate 100 stained cells were selected randomly in each experiment of (a) and were classified into 3 types "apoptosis" (green), "necrosis or late apoptosis" (both green and red) and "necrosis" (red). (For interpretation of the references to color in this figure legend, the reader is referred to the Web version of this article.)

Table 4
Protein kinase inhibition of compounds **3c**, **3f**, **3q** and erlotinib.

Kinase	IC_{50} (μM)			
	3c	**3f**	**3q**	**Erlotinib**
EGFR	23.34 ± 3.26	4.34 ± 0.66	4.71 ± 0.84	0.05 ± 0.01
HER2	6.96 ± 1.37	2.28 ± 0.53	>30	>30
HER4	1.50 ± 0.34	4.68 ± 1.12	29.02 ± 1.88	2.59 ± 0.49
IGF1R	3.28 ± 1.41	10.31 ± 2.39	>30	>30
InsR	9.79 ± 2.59	>30	>30	>30
KDR	10.50 ± 2.84	10.77 ± 2.45	25.64 ± 2.53	5.06 ± 0.69
PDGFRα	>30	>30	>30	8.12 ± 1.33
PDGFRβ	>30	>30	>30	>30

was poured into crushed ice. The precipitate was filtered and crystallized from ethanol [39].

4.1.1.2.1. 3-(4-Morpholinophenyl)-5-(4-chlorophenyl)-1-thiocarbamoyl-2-pyrazoline (2a). Yield: 85%. M.p. 199.9 °C.

IR ν_{max} (cm^{-1}): 3419.79, 3263.56 (N-H stretching), 3149.76 (aromatic C-H stretching), 2954.95, 2910.58, 2858.51 (aliphatic C-H stretching), 1606.70, 1595.13, 1577.77, 1523.76, 1467.83, 1444.68 (C=C and C=N stretching), 1350.17, 1267.23, 1234.44, 1203.58, 1122.57, 1089.78, 1056.99, 1012.63 (C=S stretching, C-N, C-O stretching and aromatic C-H in plane bending), 960.55, 925.83, 867.97, 842.89, 812.03, 781.17, 721.38, 657.73 (aromatic C-H out of plane bending).

^{1}H NMR (300 MHz, δ ppm, DMSO-d_6): 3.09 (1H, dd, J_{AB} = 17.97 Hz, J_{AX} = 3.42 Hz), 3.21 (4H, t, J = 4.68, 4.86, 9.54 Hz), 3.73 (4H, t, J = 4.26, 5.13, 9.39 Hz), 3.83 (1H, dd, J_{BA} = 17.94 Hz, J_{BX}= 11.40 Hz), 5.87 (1H, dd, J_{BX} = 11.31 Hz, J_{AX} = 3.30 Hz), 6.97 (2H, d, J = 9.06 Hz), 7.14 (2H, d, J = 8.52 Hz), 7.37 (2H, d, J = 8.49 Hz), 7.71 (2H, d, J = 8.91 Hz), 7.78 (1H, brs), 7.95 (1H, s).

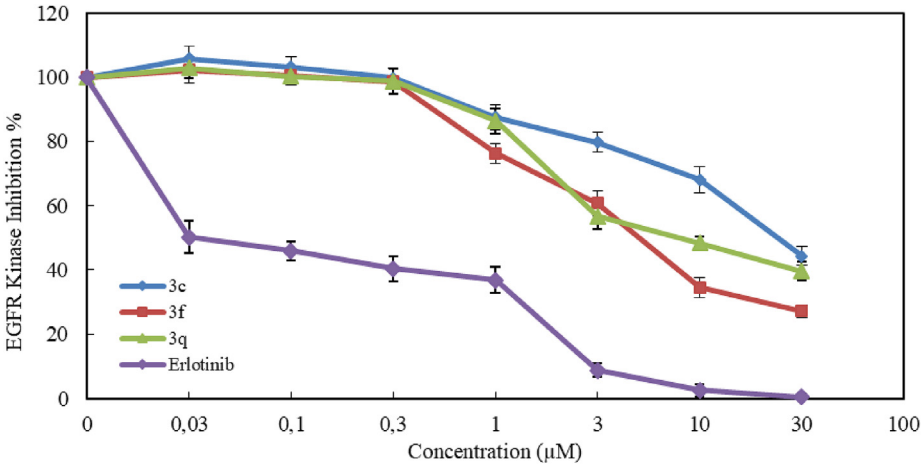

Fig. 9. The inhibitory effects of compounds **3c**, **3f**, **3q** and erlotinib on EGFR at varying concentrations.

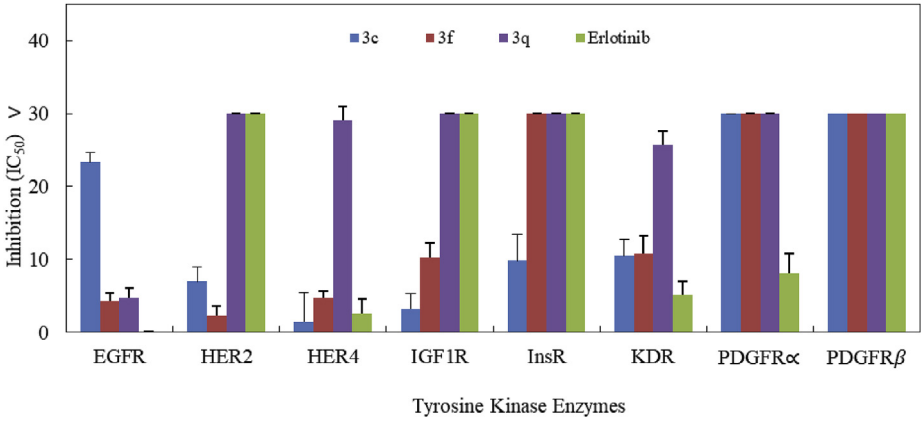

Fig. 10. The inhibition profile of compounds **3c**, **3f**, **3q** and erlotinib in the panel of eight kinases.

^{13}C NMR (75 MHz, DMSO-d_6) δ (ppm): 42.67 (CH_2), 47.78 ($2CH_2$), 62.47 (CH), 66.35 ($2CH_2$), 114.46 (2CH), 121.06 (C), 127.81 (2CH), 128.90 (4CH), 131.79 (C), 142.58 (C), 152.97 (C), 155.60 (C), 175.80 (C).

HRMS (ESI) (m/z) $[M+H]^+$ calcd. for $C_{20}H_{21}ClN_4OS$: 401.1197, found: 401.1198.

*4.1.1.2.2. 3-(4-Piperidinophenyl)-5-(4-chlorophenyl)-1-thiocarbamoyl-2-pyrazoline (**2b**).* Yield: 80%. M.p. 187.9 °C.

IR ν_{max} (cm^{-1}): 3437.15, 3273.20 (N-H stretching), 3161.33 (aromatic C-H stretching), 2929.87, 2850.79, 2812.21 (aliphatic C-H stretching), 1597.06, 1523.76, 1489.05, 1467.83, 1450.47 (C=C and C=N stretching), 1365.60, 1282.66, 1236.37, 1193.94, 1126.43, 1107.14, 1089.78, 1012.63 (C=S stretching, C-N stretching and aromatic C-H in plane bending), 954.76, 916.19, 813.96, 783.10, 700.16 (aromatic C-H out of plane bending).

^{1}H NMR (300 MHz, δ ppm, DMSO-d_6): 1.57 (10H, s), 3.07 (1H, dd, J_{AB} = 17.88 Hz, J_{AX} = 3.39 Hz), 3.82 (1H, dd, J_{BA} = 17.88 Hz, J_{BX} = 11.37 Hz), 5.87 (1H, dd, J_{BX} = 11.28 Hz, J_{AX} = 3.24, Hz), 6.93 (2H, d, J = 9.00 Hz), 7.14 (2H, d, J = 8.52 Hz), 7.36 (2H, d, J = 8.46 Hz), 7.66 (2H, d, J = 8.91 Hz), 7.72 (1H, brs), 7.89 (1H, brs).

^{13}C NMR (75 MHz, DMSO-d_6) δ (ppm): 24.41 (CH_2), 25.32 ($2CH_2$), 42.68 (CH_2), 48.74 ($2CH_2$), 62.42 (CH), 114.62 (2CH), 119.77 (C), 127.82 (2CH), 128.88 (CH), 128.97 (CH), 129.15 (CH), 129.41 (CH), 131.78 (C), 142.59 (C), 153.03 (C), 155.75 (C), 175.72 (C).

HRMS (ESI) (m/z) $[M+H]^+$ calcd. for $C_{21}H_{23}ClN_4S$: 399.1405, found: 399.1411.

*4.1.1.3. 1-(4-Arylthiazol-2-yl)-3-(4-morpholino/piperidinophenyl)-5-(4-chlorophenyl)-2-pyrazolines (**3a-v**).* A mixture of compound **2a**/**2b** (0.001 mol) and 2-bromo-1-arylethanone (0.001 mol) in ethanol (20 mL) was refluxed for 6 h. After cooling, the precipitate was collected by suction filtration. The product was crystallized from ethanol [39].

*4.1.1.3.1. 1-(4-Phenylthiazol-2-yl)-3-(4-morpholinophenyl)-5-(4-chlorophenyl)-2-pyrazoline (**3a**).* Yield: 79%. M.p. 244.6 °C.

IR ν_{max} (cm^{-1}): 3111.18, 3047.53 (aromatic C-H stretching), 2960.73, 2918.30, 2856.58, 2818.00 (aliphatic C-H stretching), 1606.70, 1541.12, 1508.33, 1479.40, 1442.75 (C=C and C=N stretching), 1427.32, 1377.17, 1327.03, 1305.81, 1294.24, 1265.30, 1256.73, 1232.51, 1217.08, 1203.58, 1089.78, 1070.49, 1053.13, 1024.20, 1014.56 (C-H bending, C-N, C-O stretching and aromatic C-H in plane bending), 925.83, 916.19, 831.32, 810.10, 781.17, 769.60, 702.09, 659.66 (aromatic C-H out of plane bending and C-S stretching).

^{1}H NMR (300 MHz, DMSO-d_6): 3.21 (4H, t, J = 4.74, 4.77, 9.51 Hz), 3.29 (1H, dd, J_{AB} = 17.73 Hz, J_{AX} = 6.51 Hz), 3.74 (4H, t, J = 4.38, 5.07, 9.45 Hz), 3.99 (1H, dd, J_{BA} = 17.73 Hz, J_{BX} = 11.73 Hz), 5.63 (1H, dd, J_{BX} = 11.82 Hz, J_{AX} = 6.63 Hz), 7.01 (2H, d, J = 9.00 Hz), 7.29 (1H, s), 7.34 (3H, t, J = 7.11, 7.74, 14.85 Hz), 7.42 (4H, s), 7.64 (2H, d, J = 8.85 Hz), 7.70 (2H, d, J = 8.49 Hz).

^{13}C NMR (75 MHz, DMSO-d_6) δ (ppm): 43.61 (CH_2), 47.94 ($2CH_2$), 63.77 (CH), 66.38 ($2CH_2$), 104.50 (CH), 114.75 (2CH), 121.42 (C), 125.93 (2CH), 127.95 (CH), 128.12 (2CH), 128.97 (4CH), 129.06 (2CH),

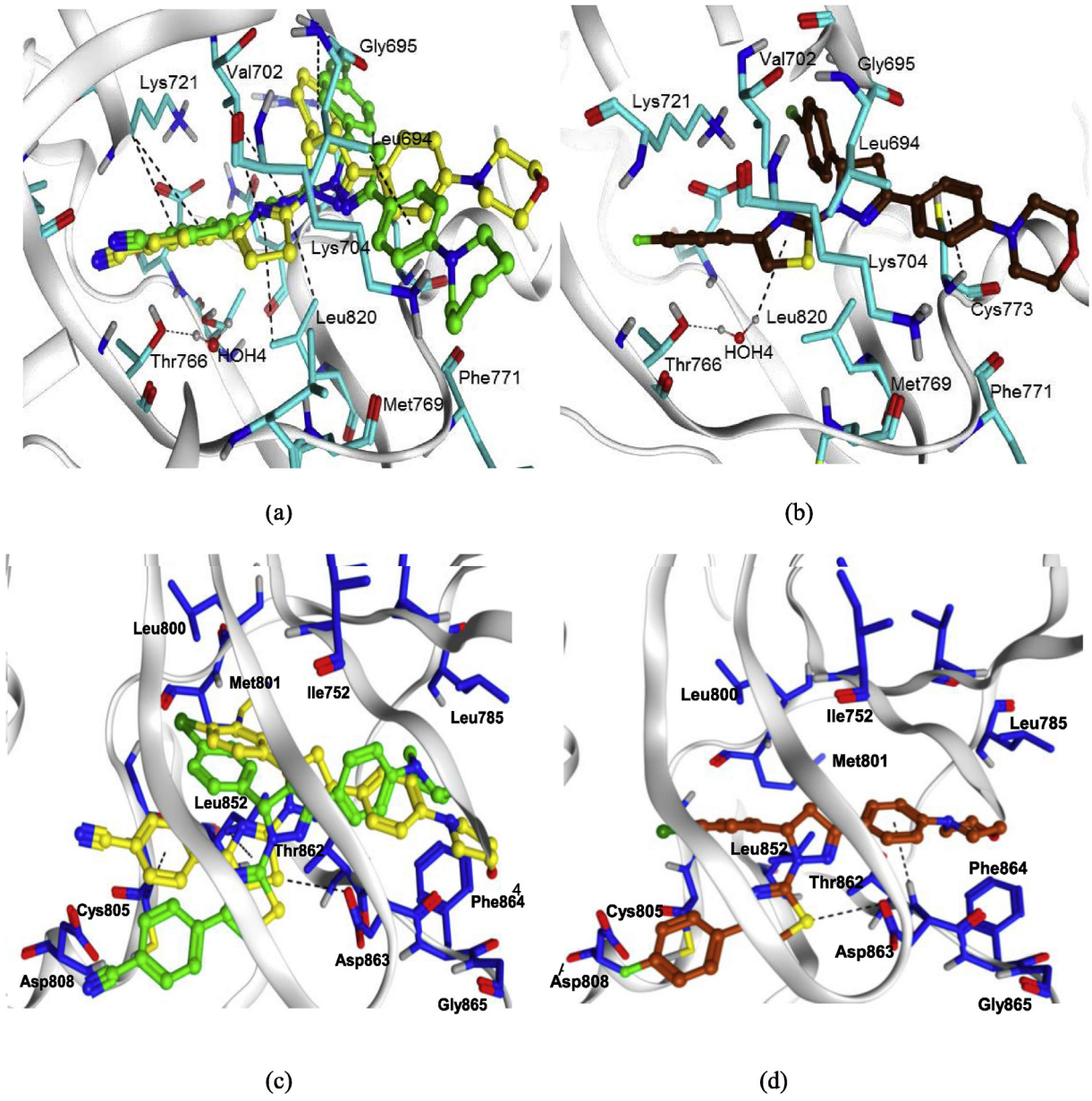

Fig. 11. Docking results of compounds **3f**, **3q** and **3c** into the active site of EGFR (PDB: 4HJO); cyan stick amino acid residue (a) and (b) and HER2 (PDB: 3RCD); blue stick amino acid residues (c) and (d): (a) Superimposed binding pose of compound **3f** and compound **3q** (yellow and green carbons; ball and stick). (b) Binding mode of compound **3c** (brown carbons; ball and stick). (c) Superimposed binding pose of compound **3f** and compound **3q** (yellow and green carbons; ball and stick). (d) Binding mode of compound **3c** (brown carbons; ball and stick); all heteroatoms are colored by element. Ligand-protein interactions are shown as black dashes. (For interpretation of the references to color in this figure legend, the reader is referred to the Web version of this article.)

132.39 (C), 134.96 (C), 141.50 (C), 150.87 (C), 152.57 (C), 153.51 (C), 164.97 (C).

HRMS (ESI) (*m/z*) $[M+H]^+$ calcd. for $C_{28}H_{25}ClN_4OS$: 501.1510, found: 501.1511.

4.1.1.3.2. 1-(4-(4-Nitrophenyl)thiazol-2-yl)-3-(4-morpholinophenyl)-5-(4-chlorophenyl)-2-pyrazoline (***3b***). Yield: 86%. M.p. 208.8 °C.

IR ν_{max} (cm^{-1}): 3105.39, 3064.89 (aromatic C-H stretching), 2968.45, 2920.23, 2852.72 (aliphatic C-H stretching), 1593.20, 1541.12, 1504.48, 1448.54 (NO_2, C=C and C=N stretching), 1381.03, 1336.67, 1315.45, 1282.66, 1257.59, 1234.44, 1201.65, 1107.14, 1089.78, 1049.28, 1012.63 (C-H bending, NO_2, C-N, C-O stretching and aromatic C-H in plane bending), 925.83, 858.32, 817.82, 715.59, 655.80 (aromatic C-H out of plane bending and C-S stretching).

^{1}H NMR (300 MHz, DMSO-d_6): 3.21 (4H, t, $J = 4.74$, 4.80, 9.54 Hz), 3.28 (1H, dd, $J_{AB} = 17.40$ Hz, $J_{AX} = 6.42$ Hz), 3.74 (4H, t, $J = 4.41$, 5.07, 9.48 Hz), 4.02 (1H, dd, $J_{BA} = 17.91$ Hz, $J_{BX} = 11.82$ Hz), 5.65 (1H, dd, $J_{BX} = 11.82$ Hz, $J_{AX} = 6.48$ Hz), 7.02 (2H, d, $J = 9.03$ Hz), 7.44 (4H, s), 7.65 (2H, d, $J = 8.91$ Hz), 7.68 (1H, s), 7.95 (2H, d, $J = 8.97$ Hz), 8.22 (2H, d, $J = 9.00$ Hz).

^{13}C NMR (75 MHz, DMSO-d_6) δ (ppm): 43.61 (CH_2), 47.90 (CH_2), 48.26 (CH_2), 63.70 (CH), 66.37 ($2CH_2$), 109.38 (CH), 114.72 (2CH), 121.22 (C), 124.50 (CH), 124.59 (CH), 126.71 (CH), 126.81 (CH), 128.21 (CH), 128.39 (CH), 129.04 (2CH), 129.16 (CH), 129.40 (CH), 132.51 (C), 140.93 (C), 141.15 (C), 146.64 (C), 148.83 (C), 152.66 (C), 154.11 (C), 165.19 (C).

HRMS (ESI) (*m/z*) $[M+H]^+$ calcd. for $C_{28}H_{24}ClN_5O_3S$: 546.1361, found: 546.1367.

*4.1.1.3.3. 1-(4-(4-Fluorophenyl)thiazol-2-yl)-3-(4-morpholinophenyl)-5-(4-chlorophenyl)-2-pyrazoline (**3c**).* Yield: 80%. M.p. 211.6 °C.

IR ν_{max} (cm^{-1}): 3082.25 (aromatic C-H stretching), 2972.31, 2920.23, 2856.58, 2835.36 (aliphatic C-H stretching), 1606.70, 1546.91, 1516.05, 1485.19, 1448.54 (C=C and C=N stretching), 1409.96, 1382.96, 1323.17, 1263.37, 1232.51, 1220.94, 1197.79, 1153.43, 1116.78, 1087.85, 1053.13, 1014.56 (C-H bending, C-N, C-O stretching and aromatic C-H in plane bending), 925.83, 842.89, 819.75, 773.46, 734.88, 698.23, 655.80 (aromatic C-H out of plane bending and C-S stretching).

^{1}H NMR (300 MHz, DMSO-d_6): 3.21 (4H, t, J = 4.02, 4.92, 8.76 Hz), 3.25–3.34 (1H, m), 3.74 (4H, t, J = 4.23, 4.74, 9.48 Hz), 4.00 (1H, dd, J_{BA} = 17.85 Hz, J_{BX} = 11.85 Hz), 5.62 (1H, dd, J_{BX} = 11.76 Hz, J_{AX} = 6.48 Hz), 7.01 (2H, d, J = 8.85 Hz), 7.13–7.21 (2H, m), 7.27 (1H, s), 7.42 (4H, s), 7.64 (2H, d, J = 8.76 Hz), 7.76–7.69 (2H, m).

^{13}C NMR (75 MHz, DMSO-d_6) δ (ppm): 43.62 (CH_2), 47.93 ($2CH_2$), 63.73 (CH), 66.37 ($2CH_2$), 104.22 (CH), 114.74 (2CH), 115.81 (2CH, d, J = 21.00 Hz), 121.38 (C), 127.83 (CH), 127.93 (CH), 128.13 (2CH), 128.99 (2CH), 129.03 (2CH), 131.57 (C), 132.40 (C), 141.45 (C), 149.82 (C), 152.59 (C), 160.40 (C), 163.44 (C), 165.05 (C).

HSQC (^{1}H NMR - ^{13}C NMR) (DMSO-d_6) δ (ppm): 3.21/47.93 (H_1/C_1), 3.25–3.34/43.62 (H_A/C_4), 3.74/66.37 (H_2/C_2), 4.00/43.62 (H_B/C_4), 5.62/63.73 (H_X/C_5).

HRMS (ESI) (m/z) $[M+H]^+$ calcd. for $C_{28}H_{24}ClFN_4OS$: 519.1416, found: 519.1408.

*4.1.1.3.4. 1-(4-(4-Chlorophenyl)thiazol-2-yl)-3-(4-morpholinophenyl)-5-(4-chlorophenyl)-2-pyrazoline (**3d**).* Yield: 82%. M.p. 187.8 °C.

IR ν_{max} (cm^{-1}): 3080.32 (aromatic C-H stretching), 2972.31, 2918.30, 2856.58 (aliphatic C-H stretching), 1606.70, 1543.05, 1512.19, 1489.05, 1473.62, 1448.54 (C=C and C=N stretching), 1402.25, 1382.96, 1323.17, 1265.30, 1232.51, 1199.72, 1172.72, 1118.71, 1087.85, 1053.13, 1010.70 (C-H bending, C-N, C-O stretching and aromatic C-H in plane bending), 923.90, 817.82, 771.53, 732.95, 655.80 (aromatic C-H out of plane bending and C-S stretching).

^{1}H NMR (300 MHz, DMSO-d_6): 3.21 (4H, t, J = 4.59, 4.77, 9.36 Hz), 3.26–3.33 (1H, m), 3.74 (4H, t, J = 4.44, 4.86, 9.30 Hz), 3.99 (1H, dd, J_{BA} = 17.73 Hz, J_{BX} = 11.73 Hz), 5.63 (1H, dd, J_{BX} = 6.54 Hz, J_{AX} = 11.22 Hz), 7.01 (2H, d, J = 9.00 Hz), 7.36 (1H, s), 7.39–7.51 (2H, m), 7.42 (4H, s), 7.64 (2H, d, J = 8.85 Hz), 7.72 (2H, d, J = 8.58 Hz).

^{13}C NMR (75 MHz, DMSO-d_6) δ (ppm): 43.61 (CH_2), 47.92 ($2CH_2$), 63.70 (CH), 66.37 ($2CH_2$), 105.29 (CH), 114.74 (2CH), 121.35 (C), 127.60 (2CH), 128.15 (2CH), 128.32 (2CH), 129.05 (4CH), 132.35 (C), 132.42 (C), 133.82 (C), 141.37 (C), 149.62 (C), 152.60 (C), 153.70 (C), 165.06 (C).

HSQC (^{1}H NMR - ^{13}C NMR) (DMSO-d_6) δ (ppm): 3.21/47.92 (H_1/C_1), 3.26–3.33/43.61 (H_A/C_4), 3.74/66.37 (H_2/C_2), 3.99/43.61 (H_B/C_4), 5.63/63.70 (H_X/C_5).

HRMS (ESI) (m/z) $[M+H]^+$ calcd. for $C_{28}H_{24}Cl_2N_4OS$: 535.1121, found: 535.1121.

*4.1.1.3.5. 1-(4-(4-Bromophenyl)thiazol-2-yl)-3-(4-morpholinophenyl)-5-(4-chlorophenyl)-2-pyrazoline (**3e**).* Yield: 83%. M.p. 189.7 °C.

IR ν_{max} (cm^{-1}): 3080.32 (aromatic C-H stretching), 2956.87, 2918.30, 2848.86 (aliphatic C-H stretching), 1606.70, 1543.05, 1514.12, 1489.05, 1473.62, 1448.54 (C=C and C=N stretching), 1402.25, 1382.96, 1323.17, 1232.51, 1199.72, 1172.72, 1118.71, 1087.85, 1053.13, 1010.70 (C-H bending, C-N, C-O stretching and aromatic C-H in plane bending), 925.83, 817.82, 773.46, 732.95, 655.80 (aromatic C-H out of plane bending and C-S stretching).

^{1}H NMR (300 MHz, DMSO-d_6): 3.20 (4H, t, J = 4.59, 4.74, 9.33 Hz), 3.28 (1H, dd, J_{AB} = 17.76 Hz, J_{AX} = 6.36 Hz), 3.74 (4H, t, J = 4.17, 5.07, 9.24 Hz), 3.99 (1H, dd, J_{BA} = 17.70 Hz, J_{BX} = 11.67, Hz), 5.62 (1H, dd, J_{BX} = 11.82 Hz, J_{AX} = 6.54 Hz), 7.00 (2H, d, J = 8.97 Hz), 7.35 (1H, s), 7.39–7.41 (2H, m), 7.41 (4H, s), 7.64 (2H, d, J = 8.85 Hz), 7.71 (2H, d, J = 8.58 Hz).

^{13}C NMR (75 MHz, DMSO-d_6) δ (ppm): 43.60 (CH_2), 47.92 ($2CH_2$), 63.70 (CH), 66.37 ($2CH_2$), 105.29 (CH), 114.73 (2CH), 121.35 (C), 127.60 (2CH), 128.14 (2CH), 128.99 (4CH), 129.04 (2CH), 132.36 (C), 132.43 (C), 133.82 (C), 141.36 (C), 149.63 (C), 152.59 (C), 153.68 (C), 165.06 (C).

HRMS (ESI) (m/z) $[M+H]^+$ calcd. for $C_{28}H_{24}BrClN_4OS$: 579.0615, found: 579.0605.

*4.1.1.3.6. 1-(4-(4-Cyanophenyl)thiazol-2-yl)-3-(4-morpholinophenyl)-5-(4-chlorophenyl)-2-pyrazoline (**3f**).* Yield: 85%. M.p. 205.5 °C.

IR ν_{max} (cm^{-1}): 3113.11, 3049.46 (aromatic C-H stretching), 2960.73, 2922.16, 2852.72, 2827.64 (aliphatic C-H stretching), 2220.07 (C≡N stretching), 1604.77, 1537.27, 1516.05, 1492.90, 1444.68 (C=C and C=N stretching), 1427.32, 1384.89, 1352.10, 1325.10, 1288.45, 1271.09, 1246.02, 1230.58, 1199.72, 1174.65, 1122.57, 1097.50, 1047.35, 1014.56 (C-H bending, C-N, C-O stretching and aromatic C-H in plane bending), 927.76, 846.75, 825.53, 802.39, 767.67, 752.24, 653.87 (aromatic C-H out of plane bending and C-S stretching).

^{1}H NMR (300 MHz, DMSO-d_6): 3.20 (4H, t, J = 4.71, 4.86, 9.15 Hz), 3.30 (1H, dd, J_{AB} = 17.70 Hz, J_{AX} = 6.33 Hz), 3.74 (4H, t, J = 4.56, 4.59, 9.48 Hz), 3.99 (1H, dd, J_{BA} = 17.76 Hz, J_{BX} = 11.73 Hz), 5.63 (1H, dd, J_{BX} = 11.82 Hz, J_{AX} = 6.51 Hz), 7.01 (2H, d, J = 9.00 Hz), 7.41 (4H, s), 7.60 (1H, s), 7.62–7.65 (2H, m), 7.80 (2H, d, J = 8.58 Hz), 7.87 (2H, d, J = 8.55 Hz).

^{13}C NMR (75 MHz, DMSO-d_6) δ (ppm): 43.66 (CH_2), 47.92 ($2CH_2$), 63.67 (CH), 66.36 ($2CH_2$), 108.35 (CH), 109.92 (C), 110.00 (CH), 114.74 (CH), 119.45 (C), 121.28 (C), 126.48 (CH), 126.56 (CH),128.19 (2CH), 129.02 (4CH), 132.47 (C), 133.07 (CH), 133.14 (CH), 139.02 (C), 141.25 (C), 149.14 (C), 152.61 (C), 153.96 (C), 165.14 (C).

HRMS (ESI) (m/z) $[M+H]^+$ calcd. for $C_{29}H_{24}ClN_5OS$: 526.1463, found: 526.1462.

*4.1.1.3.7. 1-(4-(4-Trifluoromethylphenyl)thiazol-2-yl)-3-(4-morpholinophenyl)-5-(4-chlorophenyl)-2-pyrazoline (**3g**).* Yield: 80%. M.p. 187.2 °C.

IR ν_{max} (cm^{-1}): 3124.68, 3055.24 (aromatic C-H stretching), 2960.73, 2920.23, 2895.15, 2854.65 (aliphatic C-H stretching), 1602.85, 1546.91, 1512.19, 1490.97, 1448.54 (C=C and C=N stretching), 1411.89, 1379.10, 1321.24, 1263.37, 1228.66, 1165.00, 1116.78, 1105.21, 1066.64, 1049.28, 1016.49 (C-H bending, C-N, C-O stretching and aromatic C-H in plane bending), 920.05, 850.61, 823.60, 813.96, 779.24, 771.53, 752.24, 711.73, 665.44, 651.94 (aromatic C-H out of plane bending and C-S stretching).

^{1}H NMR (300 MHz, DMSO-d_6): 3.21 (4H, t, J = 4.77, 4.80, 9.57 Hz), 3.28–3.34 (1H, m), 3.74 (4H, t, J = 4.41, 5.07, 9.48 Hz), 4.00 (1H, dd, J_{BA} = 17.73 Hz, J_{BX} = 11.70 Hz), 5.64 (1H, dd, J_{BX} = 11.82 Hz, J_{AX} = 6.54 Hz), 7.01 (2H, d, J = 9.03 Hz), 7.43 (4H, s), 7.53 (1H, s), 7.65 (2H, d, J = 8.88 Hz), 7.71 (2H, d, J = 8.31 Hz), 7.91 (2H, d, J = 8.07 Hz).

^{13}C NMR (75 MHz, DMSO-d_6) δ (ppm): 43.60 (CH_2), 47.92 ($2CH_2$), 63.73 (CH), 66.37 ($2CH_2$), 107.30 (CH), 114.73 (2CH), 121.30 (C), 126.01 (C), 126.42 (2CH), 127.12 (CH), 127.36 (CH), 128.18 (2CH), 129.00 (2CH), 129.11 (2CH), 132.46 (2C), 138.63 (C), 141.26 (C), 149.33 (C), 152.63 (C), 153.88 (C), 165.16 (C).

HSQC (^{1}H NMR - ^{13}C NMR) (DMSO-d_6) δ (ppm): 3.21/47.92 (H_1/C_1), 3.28–3.34/43.60 (H_A/C_4), 3.74/66.37 (H_2/C_2), 4.00/43.60 (H_B/C_4).

HRMS (ESI) (m/z) $[M+H]^+$ calcd. for $C_{29}H_{24}ClF_3N_4OS$: 569.1384, found: 569.1379.

*4.1.1.3.8. 1-(4-(4-Methylphenyl)thiazol-2-yl)-3-(4-morpholinophenyl)-5-(4-chlorophenyl)-2-pyrazoline (**3h**).* Yield: 78%. M.p. 203.2 °C.

IR ν_{max} (cm^{-1}): 3107.32, 3062.96 (aromatic C-H stretching), 2956.87, 2916.37, 2889.37, 2854.65, 2829.57 (aliphatic C-H

stretching), 1604.77, 1544.98, 1514.12, 1487.12, 1446.61 (C=C and C=N stretching), 1381.03, 1325.10, 1296.16, 1263.37, 1230.58, 1197.79, 1118.71, 1089.78, 1051.20, 1016.49 (C-H bending, C-N, C-O stretching and aromatic C-H in plane bending), 923.90, 821.68, 781.17, 725.23, 690.52, 655.80 (aromatic C-H out of plane bending and C-S stretching).

^{1}H NMR (300 MHz, DMSO-d_6): 2.28 (3H, s), 3.21 (4H, t, $J = 4.77$, 4.80, 9.57 Hz), 3.29 (1H, dd, $J_{AB} = 17.70$ Hz, $J_{AX} = 6.57$ Hz), 3.74 (4H, t, $J = 4.38$, 5.10, 9.48 Hz), 3.99 (1H, dd, $J_{BA} = 17.73$ Hz, $J_{BX} = 11.73$ Hz), 5.62 (1H, dd, $J_{BX} = 11.85$ Hz, $J_{AX} = 6.69$ Hz), 7.01 (2H, d, $J = 9.03$ Hz), 7.15 (2H, d, $J = 8.01$ Hz), 7.21 (1H, s), 7.42 (4H, s), 7.59 (2H, d, $J = 8.13$ Hz), 7.64 (2H, d, $J = 8.85$ Hz).

^{13}C NMR (75 MHz, DMSO-d_6) δ (ppm): 21.27 (CH_3), 43.57 (CH_2), 47.95 ($2CH_2$), 63.78 (CH), 66.38 ($2CH_2$), 103.57 (CH), 114.76 (2CH), 121.45 (C), 125.88 (2CH), 128.10 (2CH), 128.95 (2CH), 129.08 (2CH), 129.51 (2CH), 132.34 (C), 132.37 (C), 137.20 (C), 141.50 (C), 150.93 (C), 152.55 (C), 153.42 (C), 164.88 (C).

HRMS (ESI) (*m/z*) $[M+H]^+$ calcd. for $C_{29}H_{27}ClN_4OS$: 515.1667, found: 515.1660.

*4.1.1.3.9. 1-(4-(4-Methoxyphenyl)thiazol-2-yl)-3-(4-morpholinophenyl)-5-(4-chlorophenyl)-2-pyrazoline (**3i**).* Yield: 77%. M.p. 181.6 °C.

IR ν_{max} (cm^{-1}): 3088.03 (aromatic C-H stretching), 2962.66, 2910.58, 2835.36 (aliphatic C-H stretching), 1606.70, 1541.12, 1514.12, 1485.19, 1448.54 (C=C and C=N stretching), 1413.82, 1381.03, 1323.17, 1301.95, 1296.16, 1284.59, 1246.02, 1230.58, 1201.65, 1168.86, 1120.64, 1089.78, 1053.13, 1028.06, 1014.56 (C-H bending, C-N, C-O stretching and aromatic C-H in plane bending), 923.90, 821.68, 775.38, 736.81, 696.30, 657.73 (aromatic C-H out of plane bending and C-S stretching).

^{1}H NMR (300 MHz, DMSO-d_6): 3.21 (4H, t, $J = 4.74$, 4.80, 9.54 Hz), 3.28 (1H, dd, $J_{AB} = 17.73$ Hz, $J_{AX} = 6.57$ Hz), 3.73−3.75 (4H, m), 3.78 (3H, s), 3.99 (1H, dd, $J_{BA} = 17.70$ Hz, $J_{BX} = 11.73$), 5.61 (1H, dd, $J_{BX} = 11.85$ Hz, $J_{AX} = 6.72$ Hz), 6.90 (2H, d, $J = 8.91$ Hz), 6.97 (1H, d, $J = 8.94$ Hz), 7.01 (1H, d, $J = 9.00$ Hz), 7.11 (1H, s), 7.42 (4H, s), 7.62 (4H, d, $J = 9.15$ Hz).

^{13}C NMR (75 MHz, DMSO-d_6) δ (ppm): 43.58 (CH_2), 47.95 ($2CH_2$), 55.57 (CH_3), 63.79 (CH), 66.38 ($2CH_2$), 102.33 (CH), 114.32 (2CH), 114.76 (2CH), 121.47 (C), 127.26 (2CH), 127.86 (C), 128.09 (2CH), 128.96 (2CH), 129.06 (2CH), 132.36 (C), 141.55 (C), 150.72 (C), 152.54 (C), 153.37 (C), 159.21 (C), 164.90 (C).

HRMS (ESI) (*m/z*) $[M+H]^+$ calcd. for $C_{29}H_{27}ClN_4O_2S$: 531.1616, found: 531.1622.

*4.1.1.3.10. 1-(4-(4-Methylsulfonylphenyl)thiazol-2-yl)-3-(4-morpholinophenyl)-5-(4-chlorophenyl)-2-pyrazoline (**3j**).* Yield: 76%. M.p. 250.3 °C.

IR ν_{max} (cm^{-1}): 3116.97, 3062.96 (aromatic C-H stretching), 2966.52, 2924.09, 2848.86, 2825.72 (aliphatic C-H stretching), 1604.77, 1593.20, 1548.84, 1514.12, 1489.05, 1456.26 (C=C and C=N stretching), 1402.25, 1384.89, 1327.03, 1300.02, 1280.73, 1234.44, 1197.79, 1145.72, 1120.64, 1087.85, 1049.28, 1012.63 (C-H bending, C-N, C-O stretching and aromatic C-H in plane bending), 952.84, 925.83, 854.47, 813.96, 769.60, 736.81, 723.31, 702.09, 682.80, 655.80 (aromatic C-H out of plane bending and C-S stretching).

^{1}H NMR (300 MHz, DMSO-d_6): 3.20−3.23 (4H, m), 3.24 (3H, s), 3.33 (1H, dd, $J_{AB} = 17.70$ Hz, $J_{AX} = 6.45$ Hz), 3.74 (4H, t, $J = 4.32$, 5.13, 9.45 Hz), 4.01 (1H, dd, $J_{BA} = 17.73$ Hz, $J_{BX} = 11.67$ Hz), 5.64 (1H, dd, $J_{BX} = 11.82$ Hz, $J_{AX} = 6.63$ Hz), 7.02 (2H, d, $J = 9.03$ Hz), 7.43 (4H, s), 7.59 (1H, s), 7.66 (2H, d, $J = 8.29$ Hz), 7.89 (2H, d, $J = 8.76$ Hz), 7.95 (2H, d, $J = 9.08$ Hz).

^{13}C NMR (75 MHz, DMSO-d_6) δ (ppm): 43.59 (CH_2), 44.04 (CH_3), 47.92 ($2CH_2$), 63.77 (CH), 66.37 ($2CH_2$), 108.04 (CH), 114.74 (2CH), 121.28 (C), 126.47 (2CH), 127.88 (CH), 127.98 (CH), 128.19 (2CH), 129.00 (2CH), 129.19 (2CH), 132.48 (2C), 139.64 (C), 141.21 (C), 149.19 (C), 152.64 (C), 153.96 (C), 165.15 (C).

HRMS (ESI) (*m/z*) $[M+H]^+$ calcd. for $C_{29}H_{27}ClN_4O_3S_2$: 579.1286, found: 579.1280.

*4.1.1.3.11. 1-(4-(Naphth-2-yl)thiazol-2-yl)-3-(4-morpholinophenyl)-5-(4-chlorophenyl)-2-pyrazoline (**3k**).* Yield: 82%. M.p. 221.2 °C.

IR ν_{max} (cm^{-1}): 3107.32, 3049.46 (aromatic C-H stretching), 2962.66, 2920.23, 2854.65, 2818.00 (aliphatic C-H stretching), 1606.70, 1539.20, 1517.98, 1506.41, 1489.05, 1442.75 (C=C and C=N stretching), 1427.32, 1379.10, 1338.60, 1305.81, 1265.30, 1232.51, 1170.79, 1116.78, 1091.71, 1051.20, 1014.56 (C-H bending, C-N, C-O stretching and aromatic C-H in plane bending), 925.83, 860.25, 817.82, 785.03, 765.74, 748.38, 707.88, 661.58 (aromatic C-H out of plane bending and C-S stretching).

^{1}H NMR (300 MHz, DMSO-d_6): 3.18−3.20 (4H, m), 3.32 (1H, dd, $J_{AB} = 17.85$ Hz, $J_{AX} = 6.87$ Hz), 3.73 (4H, brs), 3.99 (1H, dd, $J_{BA} = 17.53$ Hz, $J_{BX} = 11.82$ Hz), 5.66 (1H, dd, $J_{BX} = 11.76$ Hz, $J_{AX} = 7.08$ Hz), 7.00 (2H, d, $J = 8.92$ Hz), 7.44 (1H, s), 7.46−7.52 (5H, m), 7.65 (2H, d, $J = 8.87$ Hz), 7.87−7.95 (5H, m), 8.18 (1H, s).

^{13}C NMR (75 MHz, DMSO-d_6) δ (ppm): 43.54 (CH_2), 47.93 ($2CH_2$), 63.98 (CH), 66.37 ($2CH_2$), 105.28 (CH), 114.75 (2CH), 121.43 (C), 124.33 (CH), 124.57 (CH), 126.42 (C), 126.91 (CH), 127.10 (CH), 128.05 (CH), 128.13 (CH), 128.33 (CH), 128.46 (CH), 128.52 (CH), 128.97 (CH), 129.34 (CH), 132.45 (CH), 132.48 (CH), 132.87 (C), 133.51 (C), 133.67 (C), 141.44 (C), 150.78 (C), 152.56 (C), 153.61 (C), 164.97 (C).

HRMS (ESI) (*m/z*) $[M+H]^+$ calcd. for $C_{32}H_{27}ClN_4OS$: 551.1667, found: 551.1687.

*4.1.1.3.12. 1-(4-Phenylthiazol-2-yl)-3-(4-piperidinophenyl)-5-(4-chlorophenyl)-2-pyrazoline (**3l**).* Yield: 77%. M.p. 117.5 °C.

IR ν_{max} (cm^{-1}): 3116.97, 3047.53 (aromatic C-H stretching), 2918.30, 2848.86, 2796.78 (aliphatic C-H stretching), 1604.77, 1544.98, 1514.12, 1489.05, 1442.75 (C=C and C=N stretching), 1386.82, 1327.03, 1307.74, 1278.81, 1236.37, 1195.87, 1126.43, 1087.85, 1070.49, 1053.13, 1024.20, 1014.56 (C-H bending, C-N stretching and aromatic C-H in plane bending), 914.26, 848.68, 821.68, 775.38, 707.88, 665.44, 648.08 (aromatic C-H out of plane bending and C-S stretching).

^{1}H NMR (500 MHz, DMSO-d_6): 1.59 (6H, s), 3.26−3.31 (5H, m), 3.99 (1H, dd, $J_{BA} = 17.50$ Hz, $J_{BX} = 12.00$ Hz), 5.63 (1H, dd, $J_{BX} = 11.50$ Hz, $J_{AX} = 6.50$ Hz), 6.99 (2H, d, $J = 9.50$ Hz), 7.25 (1H, t, $J = 7.50$, 7.00, 14.50 Hz), 7.30 (1H, s), 7.35 (2H, t, $J = 8.00$, 7.50, 15.50 Hz), 7.43 (4H, s), 7.61 (2H, d, $J = 9.00$ Hz), 7.71 (2H, d, $J = 7.75$ Hz).

^{13}C NMR (125 MHz, DMSO-d_6) δ (ppm): 24.41 (CH_2), 25.37 ($2CH_2$), 43.62 (CH_2), 48.90 ($2CH_2$), 63.72 (CH), 104.41 (CH), 114.98 (2CH), 120.24 (C), 125.93 (2CH), 127.94 (CH), 128.21 (2CH), 128.97 (2CH), 129.05 (4CH), 132.38 (C), 135.00 (C), 141.55 (C), 150.88 (C), 152.70 (C), 153.62 (C), 165.01 (C).

COSY (^{1}H NMR - ^{1}H NMR) (DMSO-d_6) δ (ppm): 1.59/3.26−3.31 (H_1/H_2), 3.26−3.31/3.99 (H_A/H_B), 3.26−3.31/5.63 (H_A/H_X), 3.99/5.63 (H_B/H_X).

HRMS (ESI) (*m/z*) $[M+2H]^{+2}$ calcd. for $C_{29}H_{27}ClN_4S$: 250.0895, found: 250.0903.

*4.1.1.3.13. 1-(4-(4-Nitrophenyl)thiazol-2-yl)-3-(4-piperidinophenyl)-5-(4-chlorophenyl)-2-pyrazoline (**3m**).* Yield: 84%. M.p. 195.2 °C.

IR ν_{max} (cm^{-1}): 3116.97, 3064.89 (aromatic C-H stretching), 2922.16, 2848.86 (aliphatic C-H stretching), 1593.20, 1573.91, 1539.20, 1504.48 (NO_2, C=C and C=N stretching), 1386.82, 1332.81, 1315.45, 1282.66, 1240.23, 1199.72, 1126.43, 1107.14, 1089.78, 1049.28, 1012.63 (C-H bending, NO_2, C-N stretching and aromatic C-H in plane bending), 921.97, 856.39, 833.25, 819.75, 715.59 (aromatic C-H out of plane bending and C-S stretching).

^{1}H NMR (300 MHz, DMSO-d_6): 1.57 (6H, s), 3.27−3.36 (5H, m), 3.99 (1H, dd, $J_{BA} = 17.79$ Hz, $J_{BX} = 11.73$ Hz), 5.63 (1H, dd,

J_{BX} = 11.55 Hz, J_{AX} = 6.18 Hz), 6.98 (2H, d, J = 8.88 Hz), 7.43 (4H, s), 7.60 (2H, d, J = 8.82 Hz), 7.67 (1H, s), 7.95 (2H, d, J = 8.91 Hz), 8.22 (2H, d, J = 8.97 Hz).

^{13}C NMR (75 MHz, DMSO-d_6) δ (ppm): 24.39 (CH_2), 25.35 ($2CH_2$), 43.62 (CH_2), 48.87 ($2CH_2$), 63.60 (CH), 109.29 (CH), 114.95 (2CH), 124.50 (2CH), 124.59 (C), 126.70 (CH), 126.80 (CH), 128.29 (2CH), 129.03 (2CH), 129.15 (2CH), 132.49 (C), 140.94 (C), 141.18 (C), 146.60 (C), 148.81 (C), 152.71 (C), 154.17 (C), 165.18 (C).

HRMS (ESI) (m/z) $[M+H]^+$ calcd. for $C_{29}H_{26}ClN_5O_2S$: 544.1569, found: 544.1585.

*4.1.1.3.14. 1-(4-(4-Fluorophenyl)thiazol-2-yl)-3-(4-piperidinophenyl)-5-(4-chlorophenyl)-2-pyrazoline (**3n**).* Yield: 79%. M.p. 144.8 °C.

IR ν_{max} (cm^{-1}): 3113.11, 3055.24 (aromatic C-H stretching), 2918.30, 2848.86 (aliphatic C-H stretching), 1604.77, 1539.20, 1514.12, 1487.12, 1450.47 (C=C and C=N stretching), 1409.96, 1384.89, 1319.31, 1290.38, 1273.02, 1236.37, 1220.94, 1195.87, 1155.36, 1124.50, 1087.85, 1051.20, 1012.63 (C-H bending, C-N stretching and aromatic C-H in plane bending), 918.12, 840.96, 819.75, 732.95, 698.23 (aromatic C-H out of plane bending and C-S stretching).

^{1}H NMR (300 MHz, DMSO-d_6): 1.58 (6H, s), 3.26–3.37 (5H, m), 3.98 (1H, dd, J_{BA} = 17.79 Hz, J_{BX} = 11.82 Hz), 5.63 (1H, dd, J_{BX} = 11.64 Hz, J_{AX} = 6.33 Hz), 6.99 (2H, d, J = 8.88 Hz), 7.19 (2H, d, J = 8.94 Hz), 7.27 (1H, s), 7.41 (4H, s), 7.60 (2H, d, J = 8.82 Hz), 7.73–7.76 (2H, m).

^{13}C NMR (75 MHz, DMSO-d_6) δ (ppm): 24.35 (CH_2), 25.33 ($2CH_2$), 43.62 (CH_2), 48.99 ($2CH_2$), 63.66 (CH), 104.15 (CH), 115.08 (CH), 115.81 (CH), 115.95 (CH), 116.07 (CH), 127.82 (C), 127.92 (C), 128.01 (CH), 128.22 (CH), 128.31 (CH), 128.99 (4CH), 129.39 (CH), 132.38 (C), 141.48 (C), 149.80 (C), 153.67 (C), 160.39 (C), 163.62 (C), 165.04 (C).

HRMS (ESI) (m/z) $[M+H]^+$ calcd. for $C_{29}H_{26}ClFN_4S$: 517.1624, found: 517.1611.

*4.1.1.3.15. 1-(4-(4-Chlorophenyl)thiazol-2-yl)-3-(4-piperidinophenyl)-5-(4-chlorophenyl)-2-pyrazoline (**3o**).* Yield: 81%. M.p. 170.0 °C.

IR ν_{max} (cm^{-1}): 3053.32 (aromatic C-H stretching), 2931.80, 2848.86 (aliphatic C-H stretching), 1604.77, 1544.98, 1514.12, 1489.05, 1473.62, 1450.47 (C=C and C=N stretching), 1400.32, 1386.82, 1350.17, 1319.31, 1290.38, 1267.23, 1236.37, 1197.79, 1122.57, 1089.78, 1051.20, 1012.63 (C-H bending, C-N stretching and aromatic C-H in plane bending), 916.19, 819.75, 767.67, 727.16, 680.87, 638.44 (aromatic C-H out of plane bending and C-S stretching).

^{1}H NMR (300 MHz, DMSO-d_6): 1.57 (6H, s), 3.25–3.36 (5H, m), 3.97 (1H, dd, J_{BA} = 17.82 Hz, J_{BX} = 11.82 Hz), 5.61 (1H, dd, J_{BX} = 11.61 Hz, J_{AX} = 6.27 Hz), 6.97 (2H, d, J = 9.00 Hz), 7.35 (1H, s), 7.39 (1H, s), 7.41 (4H, s), 7.50 (1H, t, J = 8.28, 8.52, 16.80 Hz), 7.59 (2H, d, J = 8.88 Hz), 7.87 (2H, d, J = 8.55 Hz).

^{13}C NMR (75 MHz, DMSO-d_6) δ (ppm): 24.35 (CH_2), 25.33 ($2CH_2$), 43.61 (CH_2), 48.96 ($2CH_2$), 63.61 (CH), 105.21 (CH), 115.05 (2CH), 127.60 (2CH), 127.68 (C), 128.23 (2CH), 128.32 (CH), 128.99 (2CH), 129.10 (2CH), 129.39 (CH), 132.41 (C), 133.82 (C), 134.09 (C), 141.40 (C), 149.61 (C), 152.59 (C), 153.76 (C), 165.05 (C).

HRMS (ESI) (m/z) $[M+H]^+$ calcd. for $C_{29}H_{26}Cl_2N_4S$: 533.1328, found: 533.1329.

*4.1.1.3.16. 1-(4-(4-Bromophenyl)thiazol-2-yl)-3-(4-piperidinophenyl)-5-(4-chlorophenyl)-2-pyrazoline (**3p**).* Yield: 82%. M.p. 152.8 °C.

IR ν_{max} (cm^{-1}): 3064.89 (aromatic C-H stretching), 2922.16, 2850.79 (aliphatic C-H stretching), 1604.77, 1541.12, 1512.19, 1489.05, 1471.69, 1448.54 (C=C and C=N stretching), 1396.46, 1340.53, 1321.24, 1290.38, 1236.37, 1193.94, 1118.71, 1087.85, 1068.56, 1051.20, 1008.77 (C-H bending, C-N stretching and aromatic C-H in plane bending), 912.33, 850.61, 819.75, 767.67, 725.23, 680.87, 640.37 (aromatic C-H out of plane bending and C-S stretching).

^{1}H NMR (300 MHz, DMSO-d_6): 1.57 (6H, s), 3.25–3.38 (5H, m), 3.98 (1H, dd, J_{BA} = 17.82 Hz, J_{BX} = 11.82 Hz), 5.60 (1H, dd, J_{BX} = 6.27 Hz, J_{AX} = 11.61 Hz), 6.98 (2H, d, J = 8.85 Hz), 7.36 (1H, s), 7.40 (4H, s), 7.53 (2H, d, J = 8.61 Hz), 7.58–7.67 (4H, m).

^{13}C NMR (75 MHz, DMSO-d_6) δ (ppm): 24.34 (CH_2), 25.33 ($2CH_2$), 43.59 (CH_2), 48.98 ($2CH_2$), 63.62 (CH), 105.31 (CH), 115.07 (2CH), 120.95 (C), 127.91 (CH), 127.99 (CH), 128.23 (CH), 128.32 (CH), 128.98 (CH), 129.04 (CH), 129.38 (C), 131.89 (2CH), 132.01 (CH), 132.41 (CH), 133.76 (C), 134.10 (C), 141.37 (C), 149.65 (C), 152.55 (C), 153.75 (C), 165.04 (C).

HRMS (ESI) (m/z) $[M+2H]^{+2}$ calcd. for $C_{29}H_{26}BrClN_4S$: 289.0448, found: 289.0452.

*4.1.1.3.17. 1-(4-(4-Cyanophenyl)thiazol-2-yl)-3-(4-piperidinophenyl)-5-(4-chlorophenyl)-2-pyrazoline (**3q**).* Yield: 83%. M.p. 168.9 °C.

IR ν_{max} (cm^{-1}): 3122.75, 3082.25 (aromatic C-H stretching), 2922.16, 2850.79 (aliphatic C-H stretching), 2223.92 (C≡N stretching), 1604.77, 1573.91, 1539.20, 1512.19, 1490.97, 1444.68 (C=C and C=N stretching), 1402.25, 1325.10, 1276.88, 1238.30, 1195.87, 1176.58, 1126.43, 1087.85, 1053.13, 1012.63 (C-H bending, C-N stretching and aromatic C-H in plane bending), 916.19, 825.53, 758.02, 740.67, 698.23, 665.44 (aromatic C-H out of plane bending and C-S stretching).

^{1}H NMR (300 MHz, DMSO-d_6): 1.61–1.73 (6H, m), 3.38–3.45 (5H, m), 4.02 (1H, dd, J_{BA} = 17.91 Hz, J_{BX} = 11.88 Hz), 5.67 (1H, dd, J_{BX} = 11.73 Hz, J_{AX} = 6.30 Hz), 7.42 (4H, s), 7.63 (1H, s), 7.67 (2H, d, J = 9.36 Hz), 7.74 (2H, d, J = 8.73 Hz), 7.81 (2H, d, J = 8.61 Hz), 7.88 (2H, d, J = 8.43 Hz).

^{13}C NMR (75 MHz, DMSO-d_6) δ (ppm): 23.07 (CH_2), 24.70 ($2CH_2$), 43.54 (CH_2), 51.87 ($2CH_2$), 63.84 (CH), 108.21 (CH), 108.60 (C), 117.90 (2CH), 119.45 (C), 126.48 (CH), 126.57 (CH), 128.37 (CH), 128.58 (CH), 129.05 (4CH), 129.39 (C), 132.53 (C), 132.82 (CH), 133.09 (CH), 138.94 (C), 141.13 (C), 149.14 (C), 149.31 (C), 153.43 (C), 164.95 (C).

HRMS (ESI) (m/z) $[M+H]^+$ calcd. for $C_{30}H_{26}ClN_5S$: 524.1670, found: 524.1670.

*4.1.1.3.18. 1-(4-(4-Trifluoromethylphenyl)thiazol-2-yl)-3-(4-piperidinophenyl)-5-(4-chlorophenyl)-2-pyrazoline (**3r**).* Yield. 79%. M.p. 162.0 °C.

IR ν_{max} (cm^{-1}): 3130.47, 3076.46 (aromatic C-H stretching), 2939.52, 2850.79 (aliphatic C-H stretching), 1606.70, 1550.77, 1514.12, 1489.05 (C=C and C=N stretching), 1409.96, 1319.31, 1232.51, 1163.08, 1116.78, 1105.21, 1089.78, 1066.64, 1051.20, 1014.56 (C-H bending, C-N stretching and aromatic C-H in plane bending), 920.05, 850.61, 815.09, 769.60, 752.24, 736.81, 723.31, 707.88, 680.87, 667.37, 636.51 (aromatic C-H out of plane bending and C-S stretching).

^{1}H NMR (300 MHz, DMSO-d_6): 1.58 (6H, s), 3.27–3.35 (5H, m), 3.99 (1H, dd, J_{BA} = 17.82 Hz, J_{BX} = 11.79 Hz), 5.63 (1H, dd, J_{BX} = 11.61 Hz, J_{AX} = 6.27 Hz), 6.98 (2H, d, J = 9.03 Hz), 7.42 (4H, s), 7.53 (1H, s), 7.60 (2H, d, J = 8.85 Hz), 7.69–7.72 (2H, m), 7.91 (2H, d, J = 8.07 Hz).

^{13}C NMR (75 MHz, DMSO-d_6) δ (ppm): 24.39 (CH_2), 25.35 ($2CH_2$), 43.61 (CH_2), 48.87 ($2CH_2$), 63.63 (CH), 107.21 (CH), 114.96 (2CH), 126.01 (C), 126.41 (2CH), 126.51 (C), 128.35 (2CH), 128.58 (2CH), 129.00 (2CH), 129.10 (2CH), 129.40 (C), 132.44 (C), 138.63 (C), 141.30 (C), 149.31 (C), 152.70 (C), 153.96 (C), 165.15 (C).

HRMS (ESI) (m/z) $[M+H]^+$ calcd. for $C_{30}H_{26}ClF_3N_4S$: 567.1592, found: 567.1595.

*4.1.1.3.19. 1-(4-(4-Methylphenyl)thiazol-2-yl)-3-(4-piperidinophenyl)-5-(4-chlorophenyl)-2-pyrazoline (**3s**).* Yield: 76%. M.p. 104.5 °C.

IR ν_{max} (cm^{-1}): 3118.90, 3041.74 (aromatic C-H stretching),

2927.94, 2850.79 (aliphatic C-H stretching), 1604.77, 1548.84, 1514.12, 1487.12, 1448.54 (C=C and C=N stretching), 1384.89, 1323.17, 1301.95, 1274.95, 1236.37, 1195.87, 1126.43, 1089.78, 1051.20, 1014.56 (C-H bending, C-N stretching and aromatic C-H in plane bending), 916.19, 819.75, 783.10, 727.16, 690.52, 642.30 (aromatic C-H out of plane bending and C-S stretching).

^{1}H NMR (300 MHz, DMSO-d_6): 1.59 (6H, s), 2.28 (3H, s), 3.27–3.37 (5H, m), 3.98 (1H, dd, J_{BA} = 17.82 Hz, J_{BX} = 11.85 Hz), 5.61 (1H, dd, J_{BX} = 11.67 Hz, J_{AX} = 6.42 Hz), 7.00 (2H, d, J = 8.67 Hz), 7.15 (2H, d, J = 8.04 Hz), 7.21 (1H, s), 7.42 (4H, s), 7.57–7.62 (4H, m).

^{13}C NMR (75 MHz, DMSO-d_6) δ (ppm): 21.28 (CH_3), 24.37 (CH_2), 25.34 ($2CH_2$), 43.57 (CH_2), 48.96 ($2CH_2$), 63.68 (CH), 103.49 (CH), 115.06 (2CH), 125.87 (2CH), 128.19 (2CH), 128.28 (C), 128.95 (2CH), 129.07 (2CH), 129.52 (2CH), 129.65 (C), 132.33 (C), 137.19 (2C), 141.55 (C), 150.91 (C), 153.51 (C), 164.88 (C).

HRMS (ESI) (m/z) $[M+H]^+$ calcd. for $C_{30}H_{29}ClN_4S$: 513.1874, found: 513.1873.

*4.1.1.3.20. 1-(4-(4-Methoxyphenyl)thiazol-2-yl)-3-(4-piperidinophenyl)-5-(4-chlorophenyl)-2-pyrazoline (**3t**).* Yield: 75%. M.p. 167.5 °C.

IR ν_{max} (cm^{-1}): 3120.82, 3041.74 (aromatic C-H stretching), 2918.30, 2848.86 (aliphatic C-H stretching), 1604.77, 1546.91, 1514.12, 1487.12, 1462.04, 1450.47, 1440.83 (C=C and C=N stretching), 1384.89, 1321.24, 1301.95, 1288.45, 1246.02, 1240.23, 1220.94, 1195.87, 1170.79, 1126.43, 1091.71, 1055.06, 1024.20, 1014.56 (C-H bending, C-N, C-O stretching and aromatic C-H in plane bending), 920.05, 819.75, 781.17, 734.88, 692.44, 642.30 (aromatic C-H out of plane bending and C-S stretching).

^{1}H NMR (300 MHz, DMSO-d_6): 1.58 (6H, s), 3.27–3.37 (5H, m), 3.78 (3H, s), 3.97 (1H, dd, J_{BA} = 17.73 Hz, J_{BX} = 11.79 Hz), 5.60 (1H, dd, J_{BX} = 11.61 Hz, J_{AX} = 6.45 Hz), 6.90 (2H, d, J = 8.88 Hz), 6.98 (2H, d, J = 8.97 Hz), 7.10 (1H, s), 7.41 (4H, s), 7.58–7.64 (4H, m).

^{13}C NMR (75 MHz, DMSO-d_6) δ (ppm): 24.37 (CH_2), 25.34 ($2CH_2$), 43.57 (CH_2), 48.94 ($2CH_2$), 55.56 (CH_3), 63.71 (CH), 102.25 (CH), 114.31 (2CH), 115.04 (2CH), 127.25 (2CH), 127.86 (C), 128.17 (CH), 128.27 (C), 128.95 (2CH), 129.05 (2CH), 129.38 (CH), 132.34 (C), 141.59 (C), 150.70 (C), 152.59 (C), 153.44 (C), 159.18 (C), 164.90 (C).

HRMS (ESI) (m/z) $[M+H]^+$ calcd. for $C_{30}H_{29}ClN_4OS$: 529.1823, found: 529.1806.

*4.1.1.3.21. 1-(4-(4-Methylsulfonylphenyl)thiazol-2-yl)-3-(4-piperidinophenyl)-5-(4-chlorophenyl)-2-pyrazoline (**3u**).* Yield: 74%. M.p. 191.3 °C.

IR ν_{max} (cm^{-1}): 3113.11, 3020.53 (aromatic C-H stretching), 2935.66, 2848.86 (aliphatic C-H stretching), 1604.77, 1595.13, 1546.91, 1512.19, 1490.97, 1462.04, 1446.61 (C=C and C=N stretching), 1402.25, 1327.03, 1300.02, 1280.73, 1234.44, 1203.58, 1147.65, 1124.50, 1087.85, 1055.06, 1014.56 (C-H bending, C-N stretching and aromatic C-H in plane bending), 972.12, 952.84, 908.47, 860.25, 848.68, 837.11, 817.82, 773.46, 723.31, 663.51, 642.30 (aromatic C-H out of plane bending and C-S stretching).

^{1}H NMR (300 MHz, DMSO-d_6): 1.59 (6H, s), 3.20–3.28 (5H, m), 3.32 (3H, s), 4.00 (1H, dd, J_{BA} = 17.82 Hz, J_{BX} = 11.76 Hz), 5.63 (1H, dd, J_{BX} = 11.55 Hz, J_{AX} = 6.33 Hz), 6.98 (2H, d, J = 8.91 Hz), 7.43 (4H, s), 7.57 (1H, s), 7.61 (2H, d, J = 8.79 Hz), 7.87–7.96 (4H, m).

^{13}C NMR (75 MHz, DMSO-d_6) δ (ppm): 24.40 (CH_2), 25.36 ($2CH_2$), 43.59 (CH_3), 44.05 (CH_2), 48.88 ($2CH_2$), 63.71 (CH), 107.95 (CH), 114.95 (2CH), 120.08 (C), 126.47 (CH), 126.55 (CH), 127.86 (CH), 127.98 (CH), 128.28 (CH), 128.38 (CH), 129.00 (CH), 129.17 (2CH), 129.40 (CH), 132.46 (C), 139.48 (C), 139.64 (C), 141.26 (C), 149.20 (C), 152.74 (C), 154.07 (C), 165.18 (C).

HRMS (ESI) (m/z) $[M+H]^+$ calcd. for $C_{30}H_{29}ClN_4O_2S_2$: 577.1493, found: 577.1455.

*4.1.1.3.22. 1-(4-(Naphth-2-yl)thiazol-2-yl)-3-(4-piperidinophenyl)-5-(4-chlorophenyl)-2-pyrazoline (**3v**).* Yield: 81%. M.p. 134.1 °C.

IR ν_{max} (cm^{-1}): 3051.39 (aromatic C-H stretching), 2920.23, 2848.66 (aliphatic C-H stretching), 1602.85, 1548.84, 1514.12, 1489.05, 1462.04, 1448.54 (C=C and C=N stretching), 1433.11, 1384.89, 1355.96, 1338.60, 1309.67, 1290.38, 1238.30, 1197.79, 1124.50, 1089.78, 1051.20, 1014.56 (C-H bending, C-N stretching and aromatic C-H in plane bending), 952.84, 914.26, 860.25, 815.89, 783.10, 750.31, 709.80, 644.22, 624.94 (aromatic C-H out of plane bending and C-S stretching).

^{1}H NMR (300 MHz, DMSO-d_6): 1.59 (6H, s), 3.28–3.41 (5H, m), 4.00 (1H, dd, J_{BA} = 17.76 Hz, J_{BX} = 11.73 Hz), 5.66 (1H, dd, J_{BX} = 11.52 Hz, J_{AX} = 6.66 Hz), 7.02 (2H, d, J = 8.49 Hz), 7.44 (1H, s), 7.49 (4H, s), 7.63 (2H, d, J = 8.76 Hz), 7.68–7.71 (1H, m), 7.86–7.89 (3H, m), 7.94 (2H, d, J = 8.73 Hz), 8.18 (1H, s).

^{13}C NMR (75 MHz, DMSO-d_6) δ (ppm): 24.25 (CH_2), 25.29 ($2CH_2$), 43.53 (CH_2), 49.20 ($2CH_2$), 63.90 (CH), 105.24 (CH), 115.30 (2CH), 124.32 (CH), 124.55 (CH), 126.42 (C), 126.91 (CH), 127.24 (C), 127.81 (CH), 128.05 (CH), 128.23 (CH), 128.33 (CH), 128.46 (CH), 128.52 (CH), 128.59 (CH), 128.97 (CH), 129.34 (CH), 129.40 (CH), 132.44 (C), 132.46 (C), 133.50 (C), 140.43 (C), 141.48 (C), 150.76 (C), 153.65 (C), 164.95 (C).

HRMS (ESI) (m/z) $[M+H]^+$ calcd. for $C_{33}H_{29}ClN_4S$: 549.1874, found: 549.1861.

4.2. Biochemistry

4.2.1. Cell culture and drug treatment

A549 and A375 cells were cultured in Dulbecco's Modified Eagle's medium (DMEM) (Wako Pure Chemical Industries, Osaka, Japan). MCF-7 and Jurkat cells, PBMCs (Precision Bioservices, Frederic, MD) were incubated in RPMI 1640 (Wako Pure Chemical Industries, Osaka, Japan). All media were purchased from Wako Pure Chemical Industries and supplemented with 10% fetal bovine serum (FBS) (Biosera, Kansas City, MO, USA) and 89 μM/mL streptomycin (Meiji Seika Pharma, Tokyo, Japan) in a humid atmosphere at 37 °C and 5% CO_2. In experiments, the cancer and normal cells at the concentration of 1×10^4 (for A549 and MCF-7 cells), 2×10^4 (for Jurkat cells) and 1×10^6 (for PBMCs) cells/mL were seeded into 24-well and 96-well tissue plates, respectively and then cultured for 72 h before the addition of the drugs (the optimal cell number for cytotoxicity assays was determined in preliminary experiments). The stock solutions (0.3 mM, 1 mM, 3 mM, 10 mM and 30 mM) of the compounds and erlotinib were prepared in DMSO, and the solutions were added to culture medium. The concentration of DMSO in the final culture medium was 1% [47].

4.2.2. Cytotoxicity assay

The level of cellular reduction of 3-(4,5-dimethylthiazol-2-yl)-2,5-diphenyltetrazolium bromide (MTT) (Dojindo Molecular Technologies, Kumamoto, Japan) was quantified as previously described in the literature with small modifications [48,49]. Cells were cultured in the presence of various concentrations of the tested compounds for 72 h. Cells were then stained with MTT solution and incubated for an additional 4 h at 37 °C. The solution was removed and the formazan crystals were solubilized by adding 100 μL DMSO. The absorbance of the converted dye in living cells was measured at a wavelength of 550 nm using a microplate spectrophotometer Infinitive M1000 (Tecan, Groding, Austria). Cell viability was calculated as the percentage of the viable control cells. All experiments were performed in triplicate and IC_{50} values were defined as the drug concentrations that reduced absorbance to 50% of control values.

4.2.3. Detection of cell death

After treatment of A549 and MCF-7 cells with compounds **3c**, **3f**, **3q** and erlotinib at IC_{50} concentrations for 24 h, apoptotic/necrotic/

healthy detection kit (PromoKine, Heidelberg, Germany) was performed according to PromoKine's instructions with the modifications [50]. Briefly, cells were harvested and washed with phosphate-buffered saline (PBS), then were suspended with binding buffer (1 ×). After that, 50 μL of binding buffer, 4 μL of FITC-Annexin V solution, 4 μL of ethidium homodimer III solution and 4 μL of Hoechst 33342 solution were added into the cells for 30 min at room temperature in the dark. Then, the cells were analyzed by a fluorescence microscope Biorevo Fluorescence BZ-9000 (Keyence, Osaka, Japan). The number of apoptotic cells (Annexin V), late apoptotic or necrotic cells (Annexin V and Ethidium homodimer III) and necrotic cells (Ethidium homodimer III) was determined as previously described [51].

4.2.4. Kinase inhibitory activity

Kinase selectivity profiling system assays from Promega were performed as previously described with modifications [47,52]. Multipoint dose-response experiments were performed using 8 kinases, namely EGFR, HER2, HER4, IGF1R, InsR, KDR, PDGFRα and PDGFRβ. Briefly, the kinase and substrate strips were diluted with 95 μL 2.5x Kinase Buffer and 15 μL of 100 μM ATP solutions, respectively. Kinase reactions were performed using 1 μL of the compound solution at varying concentrations (0.03 μM–30 μM), 2 μL of kinase working stock and 2 μL of ATP/substrate working stock. After 1 h incubation at room temperature, kinase activity was quantified using the ADP-Glo Kinase Assay (Promega Corporation, Madison, WI, USA). Kinase inhibition was quantified using a luminescence microplate spectrophotometer Infinitive M1000 (Tecan, Groding, Austria). The concentration of the test compounds required to decrease the kinase activity by 50% was determined using ImageJ software and identified as the IC_{50}.

4.3. Molecular modelling

EGFR and HER2 crystal structures were retrieved from PDB (accession codes: 4HJO and 3RCD, respectively). In preparation section, QuickPrep module was employed to correct structural issues, protonate, delete unnecessary water molecules, tether atoms and minimize the protein structures [53]. All preparation, docking calculations and visualization were performed using default settings implemented in MOE 2018.01 (Chemical Computing Group, Montreal, Canada) [54,55]. Ligand conformations were placed in the site with the Triangle Matcher method and ranked using the London dG scoring function. Finally, the generated poses were ranked according to their docking scores.

Acknowledgements

This study was supported by Anadolu University Scientific Research Projects Commission under the grant no: 1707S449 and the Grant-in-Aid for Challenging Exploratory Research to M.O. (24659048). A549 and MCF-7 cells were provided by the RIKEN BRC through the National Bio-Resource Project of the MEXT/AMED, Japan.

Appendix A. Supplementary data

Supplementary data to this article can be found online at https://doi.org/10.1016/j.ejmech.2019.111648.

References

[1] A. Gschwind, O.M. Fischer, A. Ullrich, The discovery of receptor tyrosine kinases: targets for cancer therapy, Nat. Rev. Cancer. 4 (2004) 361–370.
[2] Z. Du, C.M. Lovly, Mechanisms of receptor tyrosine kinase activation in cancer, Mol. Cancer. 17 (2018) 58.
[3] M.A. Lemmon, J. Schlessinger, Cell signaling by receptor tyrosine kinases, Cell 141 (2010) 1117–1134.
[4] A.I. Ségaliny, M. Tellez-Gabriel, M.F. Heymann, D. Heymann, Receptor tyrosine kinases: characterisation, mechanism of action and therapeutic interests for bone cancers, J. Bone Oncol. 4 (2015) 1–12.
[5] N.E. Hynes, H.A. Lane, ERBB receptors and cancer: the complexity of targeted inhibitors, Nat. Rev. Cancer. 5 (2005) 341–354.
[6] M. Juchum, M. Günther, S.A. Laufer, Fighting cancer drug resistance: opportunities and challenges for mutation-specific EGFR inhibitors, Drug Resist. Updates 20 (2015) 12–28.
[7] S.N. Milik, D.S. Lasheen, R.A.T. Serya, K.A.M. Abouzid, How to train your inhibitor: design strategies to overcome resistance to Epidermal Growth Factor Receptor inhibitors, Eur. J. Med. Chem. 142 (2017) 131–151.
[8] S. Giroux, Overcoming acquired resistance to kinase inhibition: the cases of EGFR, ALK and BRAF, Bioorg. Med. Chem. Lett. 23 (2013) 394–401.
[9] F. Khanjani, R.H. Sajedi, S. Hasannia, Rapid screening of drug candidates against EGFR/HER2 signaling pathway using fluorescence assay, Anal. Bioanal. Chem. 410 (2018) 7827–7835.
[10] H. Lemjabbar-Alaoui, O.U. Hassan, Y.W. Yang, P. Buchanan, Lung cancer: biology and treatment options, Biochim. Biophys. Acta 1856 (2015) 189–210.
[11] R.S. Herbst, D. Morgensztern, C. Boshoff, The biology and management of non-small cell lung cancer, Nature 553 (2018) 446–454.
[12] J. Dowell, J.D. Minna, P. Kirkpatrick, Erlotinib hydrochloride, Nat. Rev. Drug. Discov. 4 (2005) 13–14.
[13] F.R. Hirsch, G.V. Scagliotti, J.L. Mulshine, R. Kwon, W.J. Curran Jr., Y.L. Wu, L. Paz-Ares, Lung cancer: current therapies and new targeted treatments, Lancet 389 (2017) 299–311.
[14] N. Sekhon, R.A. Kumbla, M. Mita, Current trends in cancer therapy, in: A.R. Gottlieb, P.K. Mehta (Eds.), Cardio-Oncology: Principles, Prevention and Management, Academic Press, Cambridge, 2017, pp. 1–24.
[15] P. Chanvorachote, P. Chunhacha, Lung cancer metastasis, in: A. Ahmad (Ed.), Introduction to Cancer Metastasis, Academic Press, Cambridge, 2017, pp. 61–76.
[16] S. Lal, A.E. McCart Reed, X.M. de Luca, P.T. Simpson, Molecular signatures in breast cancer, Methods 131 (2017) 135–146.
[17] N. Harbeck, M. Gnant, Breast cancer, Lancet 389 (2017) 1134–1150.
[18] W. Tsuji, J.A. Plock, Breast cancer metastasis, in: A. Ahmad (Ed.), Introduction to Cancer Metastasis, Academic Press, Cambridge, 2017, pp. 13–31.
[19] Y.J. Kim, D. Sung, E. Oh, Y. Cho, T.M. Cho, L. Farrand, J.H. Seo, J.Y. Kim, Flubendazole overcomes trastuzumab resistance by targeting cancer stem-like properties and HER2 signaling in HER2-positive breast cancer, Cancer Lett. 412 (2018) 118–130.
[20] R.J. Davey, A. van der Westhuizen, N.A. Bowden, Metastatic melanoma treatment: combining old and new therapies, Crit. Rev. Oncol. Hematol. 98 (2016) 242–253.
[21] S. Singh, A. Zafar, S. Khan, I. Naseem, Towards therapeutic advances in melanoma management: an overview, Life Sci. 174 (2017) 50–58.
[22] Q. Liu, M. Das, Y. Liu, L. Huang, Targeted drug delivery to melanoma, Adv. Drug Deliv. Rev. 127 (2018) 208–221.
[23] T. Garay, E. Molnár, É. Juhász, V. László, T. Barbai, J. Dobos, K. Schelch, C. Pirker, M. Grusch, W. Berger, J. Tímár, B. Hegedűs, Sensitivity of melanoma cells to EGFR and FGFR activation but not inhibition is influenced by oncogenic BRAF and NRAS mutations, Pathol. Oncol. Res. 21 (2015) 957–968.
[24] M. Katunarić, D. Jurišić, M. Petković, M. Grahovac, B. Grahovac, G. Zamolo, EGFR and cyclin D1 in nodular melanoma: correlation with pathohistological parameters and overall survival, Melanoma Res. 24 (2014) 584–591.
[25] K.M. Qiu, H.H. Wang, L.M. Wang, Y. Luo, X.H. Yang, X.M. Wang, H.L. Zhu, Design, synthesis and biological evaluation of pyrazolyl-thiazolinone derivatives as potential EGFR and HER-2 kinase inhibitors, Bioorg. Med. Chem. 20 (2012) 2010–2018.
[26] R. Guda, G. Kumar, R. Korra, S. Balaji, G. Dayakar, R. Palabindela, P. Myadaraveni, N.R. Yellu, M. Kasula, EGFR, HER2 target based molecular docking analysis, *in vitro* screening of 2, 4, 5-trisubstituted imidazole derivatives as potential anti-oxidant and cytotoxic agents, J. Photochem. Photobiol., B 176 (2017) 69–80.
[27] X. Li, C. Yang, H. Wan, G. Zhang, J. Feng, L. Zhang, X. Chen, D. Zhong, L. Lou, W. Tao, L. Zhang, Discovery and development of pyrotinib: a novel irreversible EGFR/HER2 dual tyrosine kinase inhibitor with favorable safety profiles for the treatment of breast cancer, Eur. J. Pharm. Sci. 110 (2017) 51–61.
[28] E. Dietel, A. Brobeil, C. Tag, S. Gattenloehner, M. Wimmer, Effectiveness of EGFR/HER2-targeted drugs is influenced by the downstream interaction shifts of PTPIP51 in HER2-amplified breast cancer cells, Oncogenesis 7 (2018), 64.
[29] M.M. Ghorab, M.S. Alsaid, A.M. Soliman, Dual EGFR/HER2 inhibitors and apoptosis inducers: new benzo[*g*]quinazoline derivatives bearing benzenesulfonamide as anticancer and radiosensitizers, Bioorg. Chem. 80 (2018) 611–620.
[30] M. Hossam, D.S. Lasheen, N.S.M. Ismail, A. Esmat, A.M. Mansour, A.N.B. Singab, K.A.M. Abouzid, Discovery of anilino-furo[2,3-*d*]pyrimidine derivatives as dual inhibitors of EGFR/HER2 tyrosine kinase and their anticancer activity, Eur. J. Med. Chem. 144 (2018) 330–348.
[31] M.B. Labib, J.N. Philoppes, P.F. Lamie, E.R. Ahmed, Azole-hydrazone derivatives: design, synthesis, in vitro biological evaluation, dual EGFR/HER2 inhibitory activity, cell cycle analysis and molecular docking study as anticancer agents, Bioorg. Chem. 76 (2018) 67–80.

[32] M.R. Shaaban, A.S. Mayhoub, A.M. Farag, Recent advances in the therapeutic applications of pyrazolines, Expert Opin. Ther. Pat. 22 (2012) 253–291.
[33] J.M. Alex, R. Kumar, 4,5-Dihydro-1*H*-pyrazole: an indispensable scaffold, J. Enzym. Inhib. Med. Chem. 29 (2014) 427–442.
[34] P.S. Negi, J. Singh, G.J.N. Pant, M. Rawat, Heterocyclic compounds: 2-Pyrazolines are biological active as well as fluorescence agents, an Overview, Anti Cancer Agents Med. Chem. 18 (2018) 1366–1385.
[35] A. Leoni, A. Locatelli, R. Morigi, M. Rambaldi, Novel thiazole derivatives: a patent review (2008 - 2012; Part 1), Expert Opin. Ther. Pat. 24 (2014) 201–216.
[36] R. Morigi, A. Locatelli, A. Leoni, M. Rambaldi, Recent patents on thiazole derivatives endowed with antitumor activity, Recent Pat, Anticancer Drug Discov 10 (2015) 280–297.
[37] S. Jain, S. Pattnaik, K. Pathak, S. Kumar, D. Pathak, S. Jain, A. Vaidya, Anticancer potential of thiazole derivatives: a retrospective review, Mini Rev. Med. Chem. 18 (2018) 640–655.
[38] P.C. Lv, D.D. Li, Q.S. Li, X. Lu, Z.P. Xiao, H.L. Zhu, Synthesis, molecular docking and evaluation of thiazolyl-pyrazoline derivatives as EGFR TK inhibitors and potential anticancer agents, Bioorg. Med. Chem. Lett. 21 (2011) 5374–5377.
[39] M.D. Altıntop, A. Özdemir, G. Turan-Zitouni, S. Ilgın, Ö. Atlı, R. Demirel, Z.A. Kaplancıklı, A novel series of thiazolyl-pyrazoline derivatives: synthesis and evaluation of antifungal activity, cytotoxicity and genotoxicity, Eur. J. Med. Chem. 92 (2015) 342–352.
[40] D. Havrylyuk, O. Roman, R. Lesyk, Synthetic approaches, structure activity relationship and biological applications for pharmacologically attractive pyrazole/pyrazoline-thiazolidine-based hybrids, Eur. J. Med. Chem. 113 (2016) 145–166.
[41] B. Sever, M.D. Altıntop, H. Karaca Gencer, H.A. Kapkac, O. Atli, M. Baysal, A. Ozdemir, Synthesis of new thiazolyl-pyrazoline derivatives and evaluation of their antimicrobial, cytotoxic and genotoxic effects, Lett. Drug Des. Discov. 15 (2018) 744–756.
[42] J.H. Park, Y. Liu, M.A. Lemmon, R. Radhakrishnan, Erlotinib binds both inactive and active conformations of the EGFR tyrosine kinase domain, Biochem. J. 448 (2012) 417–423.
[43] T. Ishikawa, M. Seto, H. Banno, Y. Kawakita, M. Oorui, T. Taniguchi, Y. Ohta, T. Tamura, A. Nakayama, H. Miki, H. Kamiguchi, T. Tanaka, N. Habuka, S. Sogabe, J. Yano, K. Aertgeerts, K. Kamiyama, Design and synthesis of novel human epidermal growth factor receptor 2 (HER2)/epidermal growth factor receptor (EGFR) dual inhibitors bearing a pyrrolo[3,2-*d*]pyrimidine scaffold, J. Med. Chem. 54 (2011) 8030–8050.
[44] A. Özdemir, B. Sever, M.D. Altıntop, E. Kaya Tilki, M. Dikmen, Design, synthesis, and neuroprotective effects of a series of pyrazolines against 6-hydroxydopamine-induced oxidative stress, Molecules 23 (2018), 2151.
[45] B.S. Kurşun-Aktar, E.E. Oruç-Emre, A. Karaküçük-İyidoğan, A. Şahin Yağlıoğlu, İ. Demirtaş, Ş. Tekin, Synthesis and structure-activity relationship study: anticancer chalcones derived from 4′-morpholinoacetophenone, Marmara Pharm. J. 21 (2017) 949–960.
[46] N. Mishra, P. Arora, B. Kumar, L.C. Mishra, A. Bhattacharya, S.K. Awasthi, V.K. Bhasin, Synthesis of novel substituted 1,3-diaryl propenone derivatives and their antimalarial activity *in vitro*, Eur. J. Med. Chem. 43 (2008) 1530–1535.
[47] M.D. Altıntop, H.I. Ciftci, M.O. Radwan, B. Sever, Z.A. Kaplancıklı, T.F.S. Ali, R. Koga, M. Fujita, M. Otsuka, A. Özdemir, Design, synthesis, and biological evaluation of novel 1,3,4-thiadiazole derivatives as potential antitumor agents against chronic myelogenous leukemia: striking effect of nitrothiazole moiety, Molecules 23 (2017) 59.
[48] T.F.S. Ali, K. Iwamaru, H.I. Ciftci, R. Koga, M. Matsumoto, Y. Oba, H. Kurosaki, M. Fujita, Y. Okamoto, K. Umezawa, M. Nakao, T. Hide, K. Makino, J. Kuratsu, M. Abdel-Aziz, D. Abuo-Rahma Gel, E.A. Beshr, M. Otsuka, Novel metal chelating molecules with anticancer activity. Striking effect of the imidazole substitution of the histidine-pyridine-histidine system, Bioorg. Med. Chem. 23 (2015) 5476–5482.
[49] N. Bayrak, H. Yıldırım, A.F. Tuyun, E.M. Kara, B.O. Celik, G.K. Gupta, H.I. Ciftci, M. Fujita, M. Otsuka, H.R. Nasiri, Synthesis, computational study, and evaluation of *in vitro* antimicrobial, antibiofilm, and anticancer activities of new sulfanyl aminonaphthoquinone derivatives, Lett. Drug Des. Discov. 14 (2017) 647–661.
[50] M. Karabacak, M.D. Altıntop, H.İ. Çiftçi, R. Koga, M. Otsuka, M. Fujita, A. Özdemir, Synthesis and evaluation of new pyrazoline derivatives as potential anticancer agents, Molecules 20 (2015) 19066–19084.
[51] H. Tateishi, K. Monde, K. Anraku, R. Koga, Y. Hayashi, H.I. Ciftci, H. DeMirci, T. Higashi, K. Motoyama, H. Arima, M. Otsuka, M. Fujita, A clue to unprecedented strategy to HIV eradication: "Lock-in and apoptosis", Sci. Rep. 7 (2017), 8957.
[52] H.I. Ciftci, S.E. Ozturk, T.F.S. Ali, M.O. Radwan, H. Tateishi, R. Koga, Z. Ocak, M. Can, M. Otsuka, M. Fujita, The first pentacyclic triterpenoid gypsogenin derivative exhibiting anti-ABL1 kinase and anti-chronic myelogenous leukemia activities, Biol. Pharm. Bull. 41 (2018) 570–574.
[53] M.O. Radwan, R. Koga, T. Hida, T. Ejima, Y. Kanemaru, H. Tateishi, Y. Okamoto, J.I. Inoue, M. Fujita, M. Otsuka, Minimum structural requirements for inhibitors of the zinc finger protein TRAF6, Bioorg. Med. Chem. Lett. 29 (2019) 2162–2167.
[54] R. Koga, M.O. Radwan, T. Ejima, Y. Kanemaru, H. Tateishi, T.F.S. Ali, H.I. Ciftci, Y. Shibata, Y. Taguchi, J.I. Inoue, M. Otsuka, M. Fujita, A dithiol compound binds to the zinc finger protein TRAF6 and suppresses its ubiquitination, ChemMedChem 12 (2017) 1935–1941.
[55] M.A. Ibrahim, A.T. El-Alfy, K. Ezel, M.O. Radwan, A.G. Shilabin, A.J. Kochanowska-Karamyan, H.I. Abd-Alla, M. Otsuka, M.T. Hamann, Marine inspired 2-(5-halo-1*H*-indol-3-yl)-*N*,*N*-dimethylethanamines as modulators of serotonin receptors: an example illustrating the power of bromine as part of the uniquely marine chemical space, Mar. Drugs. 15 (2017), 248.